PONTIFICIA UNIVERSIDAD CATÓLICA DEL PERÚ

ESCUELA DE POSGRADO

OPTIMAL CONTROL FOR A PROTOTYPE OF AN ACTIVE MAGNETIC BEARING SYSTEM

Tesis para optar el grado de Magíster en ingeniería Mecatrónica

AUTOR

DANILO EDUARDO ARAGÓN AYALA

ASESORES

Ph.D. Ing. Julio Cesar Tafur Sotelo
MSc. Ing. Jesus Alan Calderón Chavarri

JURADO

Ph.D. Ing. Elizabeth Roxana Villota Cerna
Ph.D. Ing. Julio Cesar Tafur Sotelo
Dipl. Ing. Eliseo Benjamín Barriga Gamarra

LIMA - PERÚ
2017

Contents

List of Figures

List of Tables

Chapter 1

Introduction

First applications of the electromagnetic suspension principle have been in experimental physics, and suggestions to use this principle for suspending transportation vehicles for high-speed trains go back to 1937. There are various ways of designing magnetic suspensions for a contact free support, the magnetic bearing is just one of them [BCK+09].

Most bearings are used in applications involving rotation. Nowadays, the use of contact bearings solves problems in the consumer products, industrial machinery, or transportation equipment (cars, trucks, bicycles, etc). Bearings allow the transmition of power from a motor to moving parts of a rotating machine [M+92].

For a variety of rotating machines, it would be advantageous to replace the mechanical bearings for magnetic bearings, which rely on magnetic fields to perform the same functions of levitation, centering, and thrust control of the rotating parts as those performed by a mechanical bearing. An advantage of the magnetic bearings (controlled or not) against purely mechanical is that magnetic bearings are contactless [BHP12]. As a consequence these properties allow novel constructions, high speeds with the possibility of active vibration control, operation with no mechanical wear, less maintenance and therefore lower costs. On the other hand, the complexity of the active (controlled) and passive (not controlled) magnetic bearings requires more knowledge from mechanics, electronics and control [LJKA06].

The passive magnetic bearing (PMB) presents low power loss because of the absence of current, lack of active control ability and low damping stiffness [FM01, SH08]. On the other hand, active magnetic bearing (AMB) has better control ability and high stiffness, whereas it suffers from high power loss due to the biased current [JJYX09].

Scientists of the 1930s began investigating active systems using electromagnets

for high-speed ultracentrifuges. However, not controlled magnetic bearings are physically unstable and controlled systems only provide proper stiffness and damping through sophisticated controllers and algorithms. This is precisely why, until the last decade, magnetic bearings did not become a practical alternative to rolling element bearings. Today, magnetic bearing technology has become viable because of advances in microprocessing controllers that allow for confident and robust active control [CJM04].

Magnetic bearings operate contactlessly and are therefore free of lubricant and wear. They are largely immune to heat, cold and aggressive substances and are operational in vacuum. Because of their low energy losses they are suited for applications with high rotation speeds. The forces act through an air gap, which allows magnetic suspension through hermetic encapsulations [Bet00].

Problem statement

The emerging high speed machines and or high rotation energy machines require components that allow low energy losses. The oil in contact bearing has losses in high speed rotation because of viscous friction. This can be solved by using a bearing that does not have this type of energy loss. Nowadays, the magnetic bearings are widely used in high speed machines, fliers and turbines [JJYX09]. Furthermore, magnetic bearings for electric machines are coming increasingly important to be considered in industrial activities. Engines that use this technology have features like high speed, long life and free use of polluting oil, contributing to solving the problems of pollution and conservation of natural resources [SMS03].

The active magnetic bearing systems use magnetic fields to levitate and support the shaft in an air space inside the bearing [Kan03]. The use of this technology, present one emerging bearing option with major advantages in terms of lifetime and rotational speed, and also favorably integrate into high speed machine systems [PKM$^+$01].

Tesis objectives

General objetive

This thesis presents the following general objective "Design the optimal control for a prototype of an Active Magnetic Bearing system, which enables a suspension op-

eration and reduce the use of polluting oils used in mechanical bearings to preserve natural resources."

Specific objectives

Filter noise from the position sensor. Obtain a mathematical model for a magnetic bearing prototype. To design an algorithm that obtains space state of the system. Estimate the tracking error for each control algorithm. Perform the real-time program that controls the system. Analyze and test the results of the implemented control. Report results of system behavior with the implemented control. Study the behavior of a magnetic bearing prototype. Design a linear quadratic regulated (LQR) controller.

1.1 Definitions

1.1.1 Bearing

A bearing is considered a part or a unit that serves directly as an interface between the rotating and stationary parts (say, between the shaft and the housing) [KBN07]. Also, it is defined as a part that supports loads while allows relative movement between two machine elements [M$^+$92]. The example of a rolling bearing is showed in figure 1.1. They are designed for applications such as industrial gearboxes, gearboxes in wind turbines and mining equipment [SKF].

Figure 1.1: SKF high-capacity cylindrical roller bearing by author [SKF].

1.1.2   Support

A support is considered a unit that includes at least one bearing (maybe two or more), adjoining part of a housing, and possibly other parts needed for the axial fixation of the bearings, end play adjustment, etc [KBN07].

1.1.3   Types of contact bearings

According to the type of contact, the supports may be made of rolling bearings (RBs) or sliding bearings (SBs).

Rolling bearings (RBs)

A rolling bearing is a mechanical element which reduces friction between a shaft and the parts in contact by the use of rolling, that it provides support and facilitates its displacement. Depending on their function and the applied loads, the rolling elements can be: balls, cylindrical rollers, tapered roller, spherical or cylindrical rollers [M^{+}92].

RBs content themselves at low and moderate speeds with splash lubrication or with grease applied during assembly. For these reasons, small and midsize mechanisms are usually provided with RBs, which have very low friction starting from zero speed [KBN07].

Many variations on the designs of RBs are available. See table 1.1 for a comparison of the performance relative to the others [M^{+}92].

Table 1.1: Comparison of bearing types by author [M^{+}92].

Bearing type	Radial load capacity	Thrust load capacity	Misalignment capability
Single-row, deep-groove ball	Good	Fair	Fair
Double-row, deep-groove ball	Excellent	Good	Fair
Angular contact	Good	Excellent	Poor
Cylindrical roller	Excellent	Poor	Fair
Needle	Excellent	Poor	Poor
Spherical roller	Excellent	Fair/good	Excellent
Tapered roller	Excellent	Excellent	Poor

Sliding bearings (SBs)

Mechanical element that makes a sliding friction, trying to be small as possible. The reduction of the friction is performed according to the selection of materials and lubricants. Lubricants have the task of creating a sliding film that separates the two materials or avoid direct contact [M+92].

The SBs are not as good at a low speed when the machine is starting or reciprocating, because in these cases, there is mixed or boundary friction, which is accompanied by wear and increased heat generation. SBs are more sensitive to the quality of the lubricating oil and to the mode of lubrication. In many cases, they need a pressure lubrication system with filtration to maintain lubricant cleanliness [KBN07].

Figure 1.2 show SBs with an oil-impregnated porous sintered body mainly composed of metal powder. Oil is impregnated into the pores of the bearing itself, resulting in efficient lubrication inside the bearing during operation [Sli].

Figure 1.2: Slinding bearings oil-impregnated by author [Sli].

1.1.4 Magnetic permeability

Magnetic permeability, relative increase or decrease in the resultant magnetic field inside a material compared with the magnetizing field in which the given material is located; or the property of a material that is equal to the magnetic flux density B established within the material by a magnetizing field divided by the magnetic field strength H of the magnetizing field. Magnetic permeability μ (Greek mu) is thus defined as $\mu = B/H$. Magnetic flux density B is a measure of the actual magnetic field within a material considered as a concentration of magnetic field lines, or flux,

per unit cross-sectional area [G$^+$10].

1.1.5   Lorentz force

The Lorentz-force is typically used to produce the torque in electrical machines. The force at the rotor can be calculated by the LORENTZ-force formula or more visual by the right-hand rule where the thumb goes in the direction of the B-field, the forefinger in the direction of the current and the middle finger points in the direction of the force vector [Bic91].

1.1.6   Maxwell force

The Maxwell-force is best known by the magnetic suspension-technique. As an example we will take a radial bearing with two degrees of freedom as in figure 1.3. As we can see from the MAXWELL force formula only attractive forces are possible. Considering only one axis, which corresponds to one degree of freedom, we have to add a second magnetic circuit to get a symmetrical solution [Bic91].
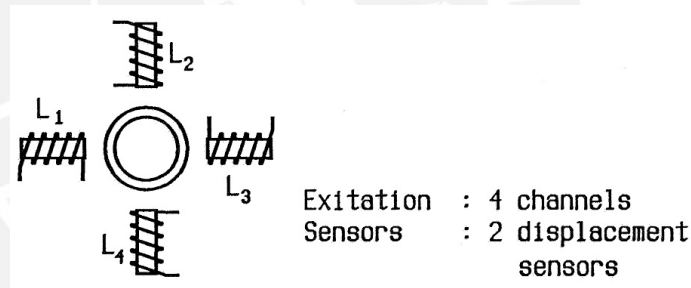
Figure 1.3: Symbolic inductors for a radial magnetic bearing with two degrees of freedom using the MAXWELL-force by author [Bic91].

1.1.7   Flotor

Flotor is a sort of coined term in this magnetic levitation idea. Instead of having a rotor in a motor that just spins [BH97]. In accordance with Hollis, Salcudean and Allan, it is proposed to call the levitated object "flotor", since it is not necessarily a rotor [SWH95, HS$^+$91].

1.1.8   Magnetic levitation

Magnetic levitation is a stable state of rest without any mechanical contact, where the gravitational force is balanced only by magnetic forces. The position of the flotor

has to remain stable when subject to "reasonable" disturbance forces. The contact free levitation should take place for all degrees of freedom of the rigid body [Ble92].

1.2 Principles of magnetic bearing functions

A sensor measures the displacement of the rotor from its reference position, a microprocessor as a controller derives a control signal from the measurement, a power amplifier transforms this control signal into a control current, and the control current generates a magnetic field in the actuating magnets, resulting in magnetic forces in such a way that the rotor remains in its hovering position. The control law of the feedback is responsible for the stability of the hovering state as well as the stiffness and the damping of such a suspension. Stiffness and damping can be varied widely within physical limits, and can be adjusted to technical requirements. They can also be changed during operation [BCK+09].

The magnetically suspended ball represents the simplest active magnetic bearing system. Unfortunately this system works just by virtue of an external force field (e.g. gravity). However all elements of a complete bearing can be found in the magnetically suspended ball too [Bet00].

Figure 1.4 shows a demonstration model for a vertical, one degree of freedom suspension. In this case the displacement of the small pencil-sharpener in the shape of a globe is measured optically by a simple photo transistor [BCK+09].
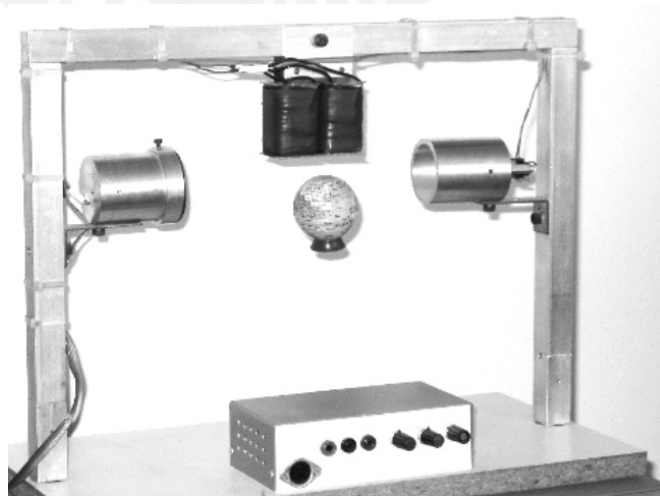
Figure 1.4: It shows a demonstration of a basic suspention. The example uses a phototransistor sensors by author [BCK+09].

1.2.1   Position sensing

The use of the different sensor families depends strongly on the media through which or on which they are to measure [Gem97]. The different measuring methods are presented in the following sections.

Optical sensor

The principle of a simple optical sensor is shown in figure 1.5. A transmitter sends a light beam towards a detector. Transmitter, detector and rotor are placed in such a way that the rotor partially interrupts the light beam. Therefore the received light quantity is a measure for the position of the rotor. Reflections interfere with this method of position sensing. Other optical techniques are based on just these reflections [Bet00].
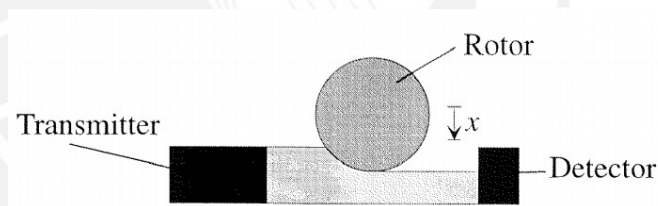
Figure 1.5: Optical sensor by author [Bet00].

Capacitive sensors

The capacity of a plate capacitor varies with its clearance. Using the capacitive measuring method, the sensor and the opposing object to be measured form one electrode of a plate capacitor each (see figure 1.6). Within the measuring system, an alternating current with a constant frequency runs through the sensor. The voltage amplitude at the sensor is proportional to the clearance between the sensor electrode and the object to be measured, and it is demodulated and amplified by a special circuit [BCK$^+$09].
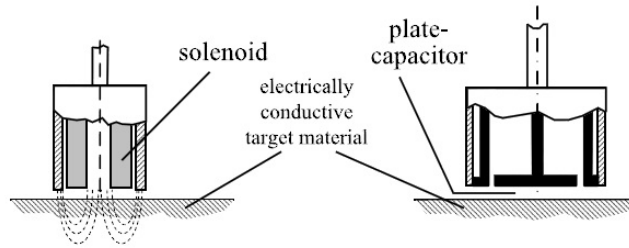
Figure 1.6: Left: eddy-current displacement sensor Right: capacitive sensor by author [BCK⁺09].

Eddy-current sensors

Eddy-current sensors are essentially built up in the same way as the inductive sensors. The two sensor types differ in the excitation frequency and the choice of the rotor material. Typically the excitation frequency lies between 100kHz and 2MHz. The rotor material should be nonmagnetic with high electrical conductivity. Usually the measurement is done on aluminium, which ideally satisfies these conditions [Bet00].

Inductive sensors

Inductive sensors consist of a coil with an alternating current passing through it (see figure 1.7). The coil is surrounded by a ferrite core. The rotor must be magnetically conducting1 at the measuring position. The impedance of the coil depends on the distance to the rotor. This can be evaluated electronically [Bet00].
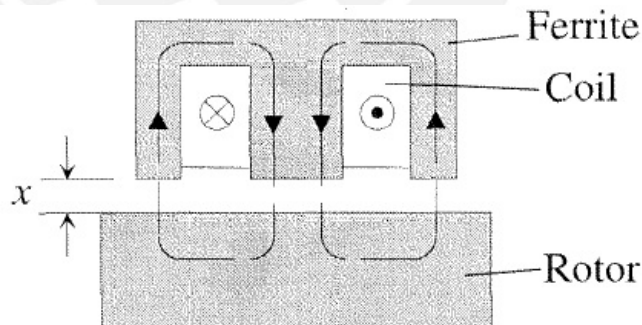
Figure 1.7: Inductive sensor by author [Bet00].

1.3   Basic types of magnetic force

A force F on an electric charge Q results according to the basic law

$$F = Q(E + v \times B) \tag{1.1}$$

with the electric field E and Q moving at velocity v in a magnetic flux density B. The complete form of Equation 1.1 was established by the dutch physicist Hendrik Antoon Lorentz(1853-1928) [Jay88].

The movement of the electric charges can be derived from the quantum effects or from a macroscopic current i. In the first case, the practice of engineering, when not dealing with the atomic or subatomic scale, has found a pleasing way of describing with quantum physics by describing the means with the magnetization constant $\mu = \mu_r \mu_0$ with μ depending on the material.

Such materials are subject to a magnetic force called here "reluctance force" to distinguish it from the "Lorentz force" obtained in the second case, with the macroscopic current i. In this case, the Lorentz force law is simplified to the familiar cross-product [Jay81].

$$F = i(l \times B) \tag{1.2}$$

The reluctance force is obtained from the principle of virtual work in arrangements of different magnetic permeability μ. The force is computed from

$$f = dW/ds \tag{1.3}$$

with the field energy W and a virtual displacement ds of the supported body [Jay88].

Table 1.2 sums up the differences of the two force types relevant inour engineering context. The "basic dependence" entries are meant to be only general relationships. The exact formulation depends very much on the given technical arrangement and various operation conditions [Ble92].

Table 1.2: The two types of magnetic force computation used in practice by author [Ble92].

	Group 1: Reluctance Force	Group 2: Lorentz Force
basic computation principle	energy in magnetic field, principle of virtual work	cross product of current and flux density
Computation formula	$f = \partial W/\partial s$	$f = i \times B$
Direction of force	perpendicular to the surface of materials of different μ_r	perpendicular to flux density
Basic dependence on current and air gap	quadratic to current inverse quadratic to air gap	linear when current and flux are no depending on each other, independent of air gap
Other pairs of names found in literature	electromagnetic alignment principle Maxwell force	electrodynamic interaction principle Lorentz force

1.4 Types of magnetic bearing

1.4.1 Magnetic bearing

It is a type of bearing that supports a load using magnetic fields to perform the functions of levitation, centering, and thrust control of the rotating parts [BHP12]. Magnetic bearings had the effect of magnetically levitating the actuation and magnetic suspension [KSI14]. An advantage of magnetic bearings compared to mechanical bearings is that they are contactless. Magnetic bearings thus require no lubrication and are not subject to wear from mechanical friction. For applications involving high rotational speed, significant energy is lost due to friction when using mechanical bearings, whereas well-designed magnetic bearings exhibit near-zero losses. Potential applications for magnetic bearings include flywheel energy storage systems for intermittent sources of renewable energy, compressors, turbines, pumps,motors, and generators [BHP12]. Compared with conventional bearings, a magnetic bearing has a lot of advantages, such as no friction, no abrasions, no lubrication, high speed, small noise, high precision, long life, and so on [LDD$^+$14].

1.4.2 Active magnetic bearings (AMBs)

The active magnetic bearing is a rotor support that uses magnetic force to hold the rotor in place as opposed to the forces of a rolling element or air foil bearing. Like other bearing types, the magnetic bearing can be characterized in terms of stiffness, damping, and load capacity, thus the forces that apply these properties are somewhat analogous for each bearing [CJM04].

In recent decades, active magnetic bearing has been widely used as a non-contact, lubrication-free, support in many industrial machines and devices [ZNTZ10].

Active magnetic bearings present one emerging bearing option with major advantages in terms of lifetime and rotational speed, and also favorably integrate into high-speed flywheel systems [PKM+01].

The active magnetic bearing presents a solution for all the technical problems of the classical bearing since it ensures the total levitation of a body in space eliminating any mechanical contact between the rotor and the stator [AO10].

As shown in figure 1.8, a magnetic bearing consists of multiple electromagnetic coils attached to a ferromagnetic stator. The coils are arranged such that opposite poles are adjacent, maximizing magnetic flux through the rotor. A ferromagnetic, laminated rotor stack is attached to the shaft to provide the flux path and attractive magnetic forces while minimizing eddy current formation [CJM04].
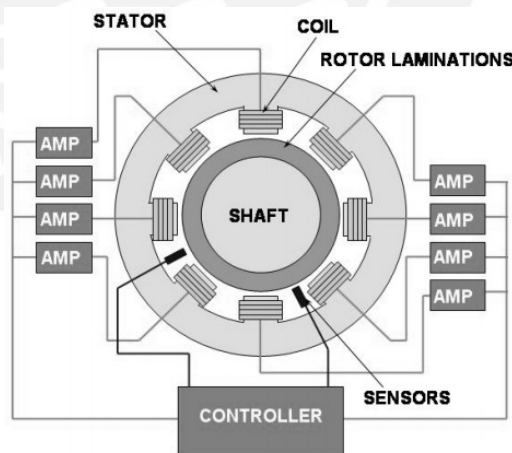
Figure 1.8: Hetero-polar magnetic bearing by author [CJM04].

1.4.3 Passive magnetic bearings (PMBs)

Passive magnetic bearings achieve contact-free levitation of an object by permanent magnetic attractive or repulsive forces. Depending on the configuration, stabilization

in radial, axial and tilt direction are possible. It is, however, not possible, to stabilized all degrees of freedom of a body by passive magnetic levitation, alone [PMB].

In addition, it can provide a high level of load capacity, stiffness, low level of rotational losses, and wide temperature operation range [FM01].

the passive magnetic bearings which can be used to provide force and torque have advantages of low loss, less number of electromagnets, simplified controller, small size, and high reliability compared with conventional AMBs [HZLX13].

An advantageous feature of passive suspension systems is that they are intrinsically stable, in contrast to active magnetic bearings and therefore can provide much higher reliability, which is known to be the crucial factor in applications requiring continuous noncontact suspension of high-speed rotors [FM01].

Compared to active magnetic bearings, passive magnetic bearings have a far lower cost [BHP13].

1.4.4 Hybrid magnetic bearings (HMBs)

The hybrid magnetic bearings combines the merits of PMB and AMB. As for HMB, the permanent magnet generates the bias flux to provide the main supporting force; consequently the control current can be reduced considerably, and the decreased control current leads to low power loss [JJYX09].

In hybrid magnetic bearing, the bias magnetic field produced by current in active magnetic bearing is replaced by permanent magnet. So power loss is decreased, the size of magnetic bearing is reduced [MYJF05].

1.5 State of art

1.5.1 Examples from industry

Areas that develop magnetic bearing technology

The various advantages of the magnetic bearing have led to applications mainly in the five following areas:

Machine tools   A main advantage is the high precision that can be attained and the high rotational speed with relatively high load capacity. This is useful for heavy-duty high speed milling of aluminum. The high speed is an essential requirement in the precision grinding of small parts [BCK+09].

Vacuum and cleanroom systems The bearings will not suffer from any mechanical wear or give rise to any related contamination, and if necessary, the bearings can even be arranged outside the vacuum container with field forces acting through the container walls. The absence of aerodynamic drag losses and the low energy consumption of the bearings is a welcome feature for flywheels for energy storage [WFDR$^+$].

Superconducting bearings The advances of superconducting bearings with their inherent passive stability promise a future alternative to active magnetic bearings. However, in order to achieve damping properties in a superconductive suspension for rotating machinery the use of additional active dampers by AMBs may still be necessary [BCK$^+$09].

Technology on market

Nowadays, there is active magnetic bearings mechatronic in the international market in several configurations.

Companies that provide active magnetic bearings

MECOS It proposes a configuration as shown in figure 1.9. It can be seen that the magnetic field enters radially and the length in the longitudinal axis is maximized by winding excel in the image [MEC15].
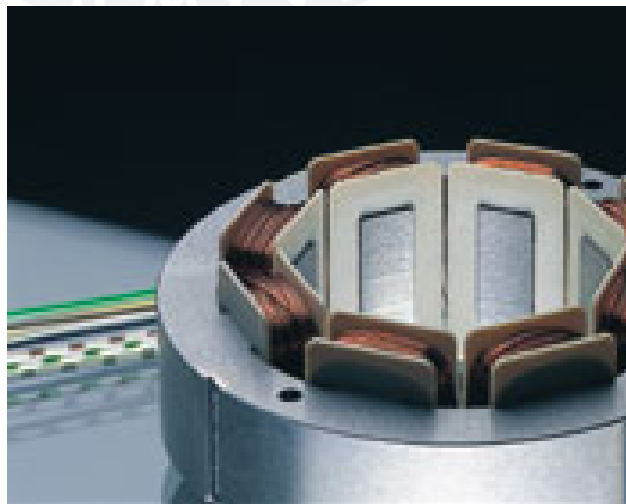
Figure 1.9: Active magnetic bearing by author [MEC15].

Levitec   The company targets the industrial sector (see Figure 1.10). In the description, describes some advantages about its active magnetic bearings: wear-free operation, has a significant reduction in life-cycle costs and minimizes maintenance intervals [Lev15]. Advantages that were discused in previous sections.

Figure 1.10: Magnetic bearing technology nowadays finds an increasing spread in the industrial sector by author [Lev15].

Synchrony Inc   Synchrony presents the benefit of using magnetic bearing (see figure 1.11). High temperature bearing Operates in process gas to a temperature of 350 °F [Syn15]. In addition, it presents the state of the of art about their magnetic bearings.

Figure 1.11: Driver for magnetic bearings by authors Victor Iannello, ScD CEO, Synchrony, Inc. [Syn15].

Each physical configuration of the actuators represents a different dynamic system modeling and control. In these three examples presented, there were obtained different mechatronic configurations. Therefore, different dynamic models and difficulty in control.

1.5.2 Examples from research projects

The examples, shown in the next figures, demonstrate recent products and developments, and an outlook on ongoing research projects.

In figure 1.12, the flywheel is on the lower left, magnetic bearing controller is at upper middle, motor generator and system controller on upper left, and motor generator power electronics on the right [BZW12].

Tesis publicada con autorización del autor
No olvide citar esta tesis

Figure 1.12: 125 kW energy storage flywheel in cabinet for UPS application and ride-through service by author [BZW12].

In figure 1.13, schematic cross-section of a turbo generator for a nuclear power plant, the first pebble-bed high temperature gas-cooled test reactor with the gas turbine in the direct cycle (HTR-10GT, under construction) [SGLY06].

Figure 1.13: Turbo generator for a nuclear power plant. The specifications are: 6 MW, 15000 rpm, vertical rotor axis, 4 radial bearings, 2 axial bearings, length of turbine 3.5 m and mass of turbine 1000 kg. By author [SGLY06].

In figure 1.14, the test rig for a superconductive bearing designed for a 4 MVA

HTS synchronous generator. In the temperature range below 60 K the bearing capacity remains almost constant. The bearing, initially cooled down to 28K, can be operated for 2 hours without additional cooling [KNN06].

Figure 1.14: Superconductive bearing. The specifications are: bearing capacity 500 kg and maximum speed 4500 rpm. By author [KNN06].

Similar research projects

Nonlinear Controllers $H\infty$ for Electromagnetic Suspension Systems

Abstract This paper presents a unified framework for deriving nonlinear status and output feedback controllers for magnetic levitation vehicles (Maglev) with controlled DC electromagnets, called electromagnetic suspension systems [SP04].

Results and conclusions The oscillating mechanism is capable of introducing a change of pitch as well as a periodic movement of the guide. The vertical profile of the guide is measured by a non-contact position sensor mounted on a fixed reference point. While linear state feedback controllers have been used successfully over the years, the new experimental results presented here demonstrate the feasibility of using more computationally demanding nonlinear controllers for the stabilization and control of electromagnetic suspension systems. The superiority of the second order state feedback and the output feedback controllers in tracking a moving guide with improved disturbance rejection properties has been developed. While both nonlinear controllers improve suspension characteristics, the output feedback controller (which

subsumes a nonlinear state estimator) has been observed to provide significant improvement over the now-classical linear state feedback controllers. The concept of linear $H\infty$ has been used for Maglev control , earlier, however, directapplication of nonlinear $H\infty$ to deal with track disturbance in an EMS system is considered to be novel [SP04].

Optimal Control of Electromagnetic Suspension EMS System

Abstract This article presents the design of the magnetic levitation application controller. The EMS system of highly non-linear electromagnetic suspension is hard and limited system control subject to the prescribed stability of the system. Due to the nonlinear dynamics of the system, the linearization of the non-linear EMS plant is described by linear model. A pulling force on the prescribed nominal operating point of the current and air gap position is chosen for linearization by a nominal operating point. An optimal control is applied to control the non-linear dynamics of the EMS plant. For this control objective the quadratic linear regulator (LQR) is applied. The stability of the system is tested using the Lyapunov method. From the results, the reference of the position of the air gap can be traced with the desired nominal operation control as shown in the simulation and in practice.

Conclusion This research proposed the control design of an EMS system of non-linear electromagnetic suspension. The linear state feedback control is designed by the linear quadratic control of the air gap position. In conclusion, the performance of the linear state feedback control system using linear quadratic regulator (LQR) can be applied to control the EMS system of non-linear electromagnetic suspension as shown in simulation and experiment. System stability and adaptation are guaranteed using the Lyapunov function candidate. The proposed control performance is stable robust [Sue14].

Control strategies for a prototype of active magnetic bearing system

Abstract Electric power in Peru is generally produced by converting mechanical energy from strong flowing rivers and flowing winds. However, when the rotor makes a maximum power, it loses power by heating, contact with the cushions also the evacuated heat affects the environmental thermal conditions (local population, animals and plants). On the other hand, a poor positioning of the rotor causes its imbalance. For this reason in this work, some control strategies are proposed to achieve

a position and velocity controller by the active mechanism: Active Magnetic Bearing (AMB). In addition, environmental protection is guaranteed due to the absence of friction between the rotor and the bearing.

Conclusion   In this work, it is proposed a methodology to achieve a good control of the position of the rotor, which is filtering the AWGN by a predictive filter. The filter designed in this paper has analyzed the least mean squares (LMS) and feedback / feedforward algorithm. The application methodology can be applied for hydraulic electric generator or electric wind generator. However, the second case could be more useful, due to an intense unstable movement caused by the winds. The controller Designed to reject noise and disturbances, although the physical identification properties are cleared out of the control algorithm [CAP+16].

Chapter 2

Mathematical modeling of the active magnetic bearing system

One of the principal objectives of this thesis is to obtain a mathematical model for a magnetic bearing prototype, which is shown in the Figure 2.1.
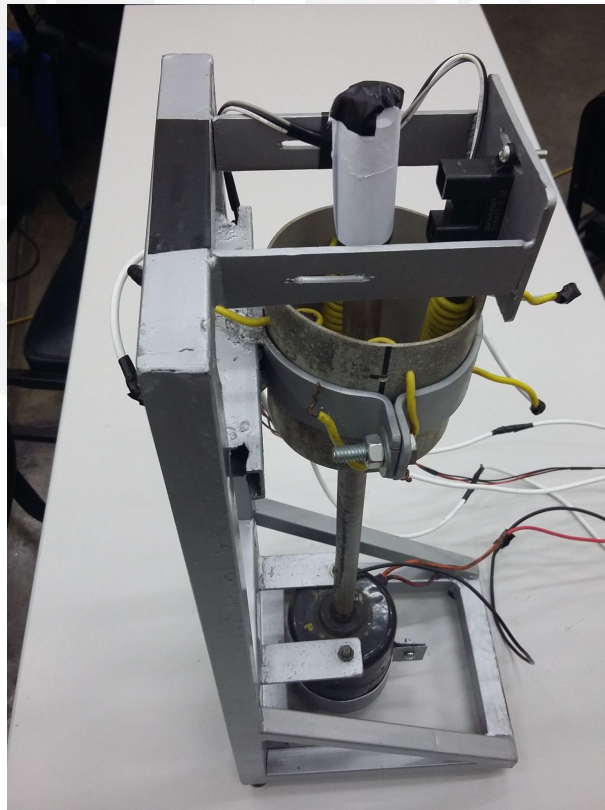
Figure 2.1: Active magnetic bearing prototype.

Figure 2.2 indicates the active magnetic bearing in the prototype and figure 2.3

shows a side cut in the 3D model of the magnetic bearing.

This view of the active magnetic bearing in detailed in figure 2.4. A basic model was developed by [Sue14]. Therefore, chapter 2 will propose two mathematical models in order to control the active magnetic bearing (AMB).
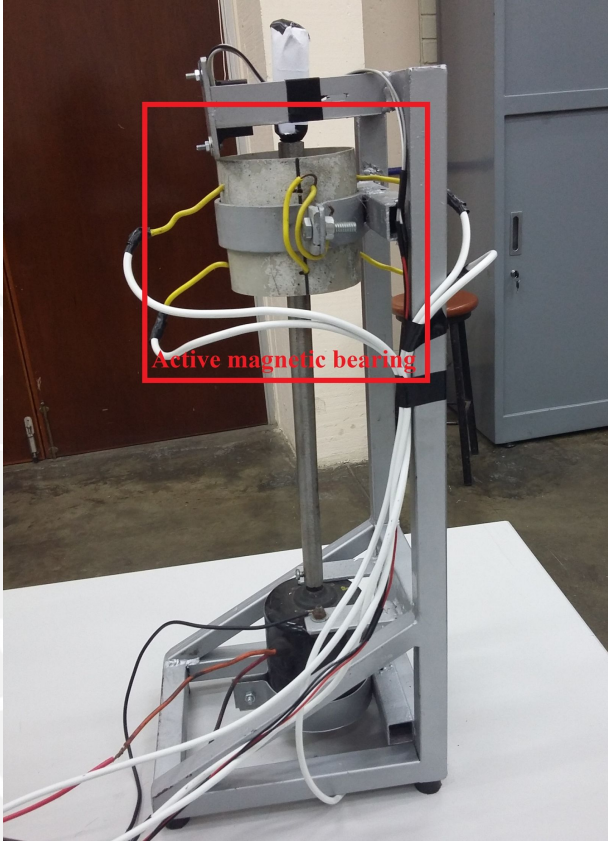
Figure 2.2: Active magnetic bearing in the prototype.
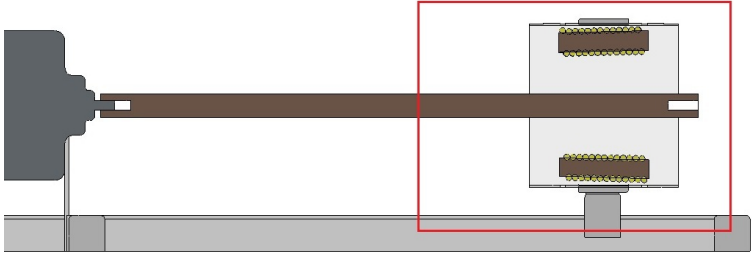
Figure 2.3: Section of the active magnetic bearing 3D model. The selected area is evaluated in the next figure.
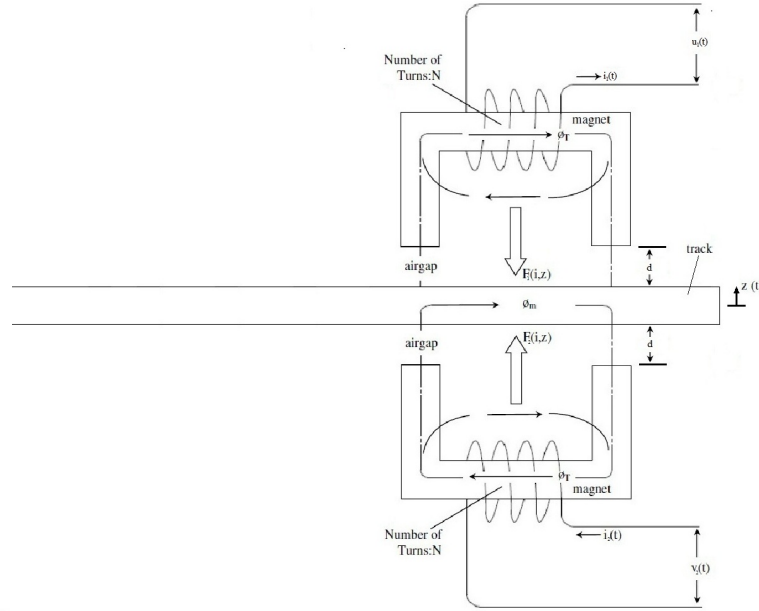
Figure 2.4: Electromagnetic suspension (EMS) system of ferromagnetic guide flotor and electromagnet coil configuration is presented. The image is modified from author [Sue14].

2.1 Active magnetic bearings

The term active implies that bearing forces are actively controlled by means of electromagnets, a suitable feedback control loop and other elements such as sensors and power amplifiers. In contrast to this architecture, a purely passive suspension produces bearing forces generated by permanent magnets acting alone. The reason for this preference of active magnetic bearings over their passive counterparts immediately becomes clear when the advantages and disadvantages in terms of bearing properties are compared. As a main advantage, active magnetic bearings feature capabilities that are freely (within the physical limitations, though) adjustable by the control, whereas passive magnetic bearings have a fixed set of properties given by their size and mechanical design. Typical examples of adjustable bearing parameters and additional capabilities of active magnetic bearings are static and dynamic stiffness, damping, load-independent static positioning, unbalance force attenuation in rotating systems, excitation force generation and monitoring, to name only a few.

2.2 Properties of ferromagnetic material

When a magnetic field with a density H acts on a material, the magnetic flux density B generated will be either higher or lower than the flux density $\mu_0 H$ generated in
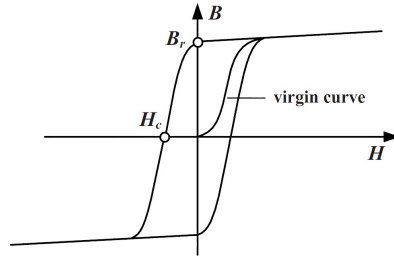
Figure 2.5: B-H diagram, hysteresis loop by author [BCK$^+$09].

the vacuum, depending on material properties. The part of B originating from the material itself is called magnetic polarization M:

$$B = \mu_0 H + M \tag{2.1}$$

Comparing 2.1 with $B = \mu_0 \mu_r H$ yields

$$M = (\mu_r - 1)H \tag{2.2}$$

in which $x_m = \mu_r - 1$ is called the magnetic susceptibility. This describes the relationship between the magnetic polarization and the flux density of the vacuum.

2.3   Magnetic Circuit

For the computation of flux density B, the following simplifying assumptions are made: Flux ϕ_r runs entirely within the magnetic loop with iron cross section A_{fe} which is assumed to be constant along the entire loop and equal to cross-section A_a in the air gap. From

$$\phi_r = B_{fe} A_{fe} = B_a A_a, \tag{2.3}$$

$$A_{fe} = A_a, \tag{2.4}$$

$$B_{fe} = B_a = B. \tag{2.5}$$

We have the area constant from equation 2.4 and therefore the magnetic flux constant 2.5. The field within the magnetic loop is assumed to be homogeneous both in the iron and in the air gap. Therefore, we base our calculation on a mean length $l_f e$ of the magnetic path and an air gap length of $2s$.

2.3.1 Flux Density Assuming Constant Permeability in the Iron

From B-H diagram we consider 2.6 and then 2.7.

$$\oint H ds = l_{fe} H_{fe} + 2s H_a = ni, \tag{2.6}$$

$$l_{fe} \frac{B}{\mu_0 \mu_r} + 2s \frac{B}{\mu_0} = ni = NI. \tag{2.7}$$

Solving 2.7 for B yields

$$B = \mu_0 \frac{NI}{\frac{l_{fe}}{\mu_r} + 2s}. \tag{2.8}$$

In the iron, $\mu_r >> 1$, so the magnetization of the iron is often neglected. In this case, 2.9 may be simplified:

$$B = \mu_0 \frac{NI}{2s}. \tag{2.9}$$

2.4 Magnetic force

In this approach, the magnet-coil has been excited by a controlled current source, which is a simpler second order transfer function for the system [1]. If N is number of turns of coil, $i(t)$ is instantaneous current through the coil, ϕ_r is total flux, R is reluctance of entire magnetic circuit, $L(z)$ is the inductance of the coil at a particular value of air-gap length (z) and z is airgap length between actuator and guide-way then. The force linkage as shown figure 2.4. is given as equation 2.10, where $L(z)$ is given as equation 2.11.

$$F(i, z, t) = -\frac{d}{dt} [\frac{1}{2} L(z) i(t)^2] \tag{2.10}$$

$$L(z) = \frac{N}{i(t)} \phi_r \tag{2.11}$$

2.5 Mathematical model

2.5.1 Complete model

Figure 2.4 shows the schematic diagram of the electromagnetic suspension (EMS) system of the one degree of freedom prototype with two controlled DC electromagnets.

The flux is generated by the electrode coil and passes through the fixation ferromagnetic track, since the inductance of the coil is calculated by [Sue14].

If reluctance of the magnetic core is neglected when applied to two air spaces, then the inductance of the coil is expressed as 2.12 with a total magnet length equal to $2z(t)$.

$$L(z) = \frac{\mu_0 N^2 A}{2z(t)} \tag{2.12}$$

Where $z(t)$ is the air gap between the magnetic pole and the ferromagnetic path. The force of attraction between the coil of the magnet and the ferromagnetic rail is given by 2.10.

Inductance form 2.12 is substituted into 2.10, we can obtained the force attraction by 2.13.

$$F(i, z, t) = \frac{\mu_0 N^2 A}{4} [\frac{i(t)}{z(t)}]^2 \tag{2.13}$$

According to the annotations given in figure 2.4, the dynamics is described by 2.12 since its motion is governed by the dynamic differential equations of motion of the electromagnetic suspension system at 2.11, 2.12 and 2.10 respectively, which refer to the dynamic movement of the rotor where the magnetic bearing is placed.

$$m\frac{d^2 z(t)}{dt} = -F_1(i_1, z + d, t) + F_2(i_2, (d - z), t) + f_d + mg - kz(t) \tag{2.14}$$

Where $F(i, z, t)$ is the electromagnetic force attraction f_d is force disturbance and d the airgap. By substituting $-\frac{\mu_0 N^2 A}{4}[\frac{i_1(t)}{(z+d)}]^2$ and $-\frac{\mu_0 N^2 A}{4}[\frac{i_2(t)}{(d-z)}]^2$ into 2.14, the equation of motion can be rearranged in 2.15.

$$m\frac{d^2 z(t)}{dt} = -kz(t) - \frac{\mu_0 N^2 A}{4}[\frac{i_1(t)}{(d+z)}]^2 + \frac{\mu_0 N^2 A}{4}[\frac{i_2(t)}{(d-z)}]^2 + f_d + mg \tag{2.15}$$

We can consider F_m the equivalent magnetic force as equation 2.16.

$$F_m = f_{m2} - f_{m1} = \frac{\mu_0 N^2 A}{4} [\frac{i_2(t)}{(d-z)}]^2 - \frac{\mu_0 N^2 A}{4} [\frac{i_1(t)}{(d+z)}]^2 \qquad (2.16)$$

The relation between the voltage $v(t)$ that varies in time through an inductor with inductance L and the variable current in time $i(t)$ that passes through it is described by the differential equation.

The electromotive force Θ is

$$\Theta = Ni \qquad (2.17)$$

Thus the flux ϕ_{fc} produced through the electromagnet coil is

$$\phi_{fc} = \frac{\Theta}{R_T} \qquad (2.18)$$

With R_T as the total reluctance of the electromagnet circuit comprising the reluctance of the magnet core, the levitated object, the air gap and the leakage flows. Reluctance is the function of the geometric and magnetic parameter by [GKTK11]. The flux linkage Ψ of the electromagnetic coil is expressed at 2.19.

$$\Psi = N\Theta_{fc} \qquad (2.19)$$

The electromagnetic suspension model of the magnetic coil with N turns is the result of the application of voltage $v(t)$ through the terminal of the coil and the current $i(t)$ produce the magnetic field in the air gap between the core of the magnet and the ferromagnetic track .

The reluctances comprise the reluctance of the magnetic core R_{fc}, the reluctance of the R_{fo} levitated object, the reluctance of the air gap R_g, and the reluctance of the R_l leakage flows. Reluctance is the function of the geometric and magnetic parameter expressed in 2.20.

$$R_T = R_{fc} + \frac{R_l(R_g + R_{f0})}{R_l + R_g + R_{f0}} \qquad (2.20)$$

Where $R_{fc} = \frac{l_{fc}}{\mu_0 \mu_r A_{fc}}$ is reluctance of the core.

$R_{f0} = \frac{l_{f0}}{\mu_0 \mu_r A_{f0}}$ is reluctance of the levitated object.

$R_g = \frac{z}{\mu_0 A_g}$ is reluctance of air gap.

$R_l = \frac{l_l}{\mu_0 \mu_r A_l}$ is the leakage reluctance.

For both circuits

$$\frac{d}{dt}\Theta_1 = -Ri_1(t) + v_1(t) \qquad (2.21)$$

and

$$\frac{d}{dt}\Theta_2 = -Ri_2(t) + v_2(t) \tag{2.22}$$

Or

$$v_1(t) = Ri_1(t) + \frac{d}{dt}\Theta_1 \tag{2.23}$$

$$v_2(t) = Ri_2(t) + \frac{d}{dt}\Theta_2 \tag{2.24}$$

Where R is an electrical resistance of circuit. $i_1(t)$ and $i_2(t)$ are the currents of both circuit. $v_1(t)$ and $v_2(t)$ are the applied voltage to both circuit. Flux linkage Θ is the function of current and position of levitated object and it can be expressed by the relationships in partial differentiation as described in 2.25.

$$\frac{d}{dt}\Theta = \frac{d\Theta}{dt}\frac{di}{dt} + \frac{d\Theta}{ds}w = L(z)\frac{di}{dt} + \frac{dL(z)}{dz}wi \tag{2.25}$$

Substitutes flux linkage into 2.25, it can be expressed as 2.26 and 2.27.

$$\frac{di_1}{dt} = \frac{1}{L(z)}(-Ri_1(t) - \frac{dL(z)}{dz}w_1i_1 + v_1(t)) \tag{2.26}$$

$$\frac{di_2}{dt} = \frac{1}{L(z)}(-Ri_2(t) - \frac{dL(z)}{dz}w_2i_2 + v_2(t)) \tag{2.27}$$

With w as the velocity of levitated object, which is $\dot{z}$. The differentiation of instantaneous current with respect to time caused by the voltage induce the coil as 2.26 and 2.27 to produce the magnetic fields by each inductance L between fix ferromagnetic guide way and magnet core and coil. The inductance is the function of position of levitated object which is found in 2.12. By substituting 2.12 into 2.26, it results in the electrical circuit of electromagnetic with applied input voltage in 2.28 across the circuit as indicate the state of current can be found as follows;

$$\frac{di_1(t)}{dt} = \frac{i_1(t)}{z(t)+d}\frac{dz(t)}{dt} - \frac{2}{\mu_0 N^2 A}(z(t)+d)(Ri_1(t) - u_1(t))) \tag{2.28}$$

$$\frac{di_2(t)}{dt} = \frac{i_2(t)}{d-z(t)}\frac{dz(t)}{dt} - \frac{2}{\mu_0 N^2 A}(d-z(t))(Ri_2(t) - u_2(t))) \tag{2.29}$$

From the differential equations of motion of nonlinear electromagnetic suspension system in 2.11 and 2.28, it converts to nonlinear state-space form in 2.5.1. The state vector can be defined as $x(t) = [z(t)\dot{z}(t)i(t)]^T \in R^2, n = 3$. The state variables, $x_1 = z(t)$ and $x_2 = \dot{z}(t)$, are the position and velocity of electromagnetic suspension coil respectively. With $x_3 = i_1(t)$ and $x_4 = i_2(t)$ are the current of each electromagnetic coil.

$$\dot{x}_1 = x_2(t)$$

$$\dot{x}_2 = -\frac{kx_1(t)}{m} - \frac{\mu_0 N^2 A}{4m}\left(\frac{x_3(t)}{x_1(t)+d}\right)^2 + \frac{\mu_0 N^2 A}{4m}\left(\frac{x_4(t)}{d-x_1(t)}\right)^2 + f_d + g$$

$$\dot{x}_3 = \frac{x_2(t)x_3(t)}{x_1(t)+d} - \frac{2R}{\mu_0 N^2 A}(x_1(t)+d)x_3(t) + \frac{2(x_1(t)+d)}{\mu_0 N^2 A}u_1(t)$$

$$\dot{x}_4 = \frac{x_2(t)x_3(t)}{d-x_1(t)} - \frac{2R}{\mu_0 N^2 A}(d-x_1(t))x_3(t) + \frac{2(d-x_1(t))}{\mu_0 N^2 A}u_2(t)$$

$$y = x_1(t) \tag{2.30}$$

If the system flotor is in the vertical position, $g = 0$ for the analysis. Then, the sistem is reduces as:

$$
\begin{bmatrix} \dot{x}_1 \\ \dot{x}_2 \\ \dot{x}_3 \\ \dot{x}_4 \end{bmatrix} = \begin{bmatrix} x_2(t) \\ -\frac{kx_1(t)}{m} - \frac{\mu_0 N^2 A}{4m}\left(\frac{x_3(t)}{x_1(t)+d}\right)^2 + \frac{\mu_0 N^2 A}{4m}\left(\frac{x_4(t)}{d-x_1(t)}\right)^2 \\ -\frac{2R(x_1(t)+d)x_3(t)}{\mu_0 N^2 A} + \frac{x_2(t)x_3(t)}{x_1(t)+d} \\ -\frac{2R(d-x_1(t))x_4(t)}{\mu_0 N^2 A} + \frac{x_2(t)x_4(t)}{d-x_1(t)} \end{bmatrix} + \begin{bmatrix} 0 & 0 \\ 0 & 0 \\ \frac{2(x_1(t)+d)}{\mu_0 N^2 A} & 0 \\ 0 & \frac{2(d-x_1(t))}{\mu_0 N^2 A} \end{bmatrix} \begin{bmatrix} u_1(t) \\ u_2(t) \end{bmatrix}
$$
$$\tag{2.31}$$

Where

$$\begin{bmatrix} x_1 \\ x_2 \\ x_3 \\ x_4 \end{bmatrix} = \begin{bmatrix} z \\ \dot{z} \\ i_1 \\ i_2 \end{bmatrix} \tag{2.32}$$

with

$$y = \begin{bmatrix} 1 & 0 & 0 & 0 \end{bmatrix} \begin{bmatrix} x_1 \\ x_2 \\ x_3 \\ x_4 \end{bmatrix} \tag{2.33}$$

.

Linearization of nonlinear electromagnetic suspension

Linearization of nonlinear electromagnetic suspension system is defined with the suitable stability of an equilibrium point. From figure 2.4, the vertical dynamic of a single degree of freedom of an electromagnetic suspension system is obtained by linearization method. The equilibrium points of the system are derived from the system equation 2.34 to the equilibrium point in 2.35.

$$\dot{x} = f(x) \tag{2.34}$$

$$z_0 = 0, \dot{z}_0 = 0, i_{10} = i_{20}, i_{10} = \frac{u_{10}}{R}, i_{20} = \frac{u_{20}}{R}. \tag{2.35}$$

The linearization of the system from 2.30 or 2.31 around a nominal equilibrium point $(i_{10}, z_{10}, i_{20}, \dot{z}_{10})$ has become to [Sin87].

$$
\begin{bmatrix} \dot{x}_1 \\ \dot{x}_2 \\ \dot{x}_3 \\ \dot{x}_4 \end{bmatrix} =
\begin{bmatrix}
0 & 1 & 0 & 0 \\
-\frac{k}{m} + \left(\frac{\mu_0 N^2 A}{2m}\right)\frac{i_{10}^2}{(z_0+d)^3} + \left(\frac{\mu_0 N^2 A}{2m}\right)\frac{i_{20}^2}{(d-z_0)^3} & 0 & -\frac{\mu_0 N^2 A}{2m}\frac{i_{10}}{(z_0+d)^2} & -\frac{\mu_0 N^2 A}{2m}\frac{i_{20}}{(d-z_0)^2} \\
-\frac{2(Ri_{10}-u_{10})}{\mu_0 N^2 A} - \frac{i_{10}z_0}{(z_0+d)^2} & \frac{i_{10}}{z_0+d} & \frac{z_0}{(z_0+d)^2} - \frac{2R(z_0+d)}{\mu_0 N^2 A} & 0 \\
\frac{2(Ri_{20}-u_{20})}{\mu_0 N^2 A} + \frac{i_{20}z_0}{(d-z_0)^2} & \frac{i_{20}}{d-z_0} & 0 & \frac{z_0}{(d-z_0)^2} - \frac{2R(d-z_0)}{\mu_0 N^2 A}
\end{bmatrix}
\begin{bmatrix} x_1 \\ x_2 \\ x_3 \\ x_4 \end{bmatrix}
+
\begin{bmatrix}
0 & 0 \\
0 & 0 \\
\frac{2(z_0+d)}{\mu_0 N^2 A} & 0 \\
0 & \frac{2(d-z_0)}{\mu_0 N^2 A}
\end{bmatrix}
\begin{bmatrix} u_1 & u_2 \end{bmatrix}
+
\begin{bmatrix} 0 \\ \frac{1}{m} \\ 0 \\ 0 \end{bmatrix} F_{ext}
\tag{2.36}
$$

Where F_{ext}, $u_1(t) = v_1(t)$ and $u_2(t) = v_2(t)$ are defined as inputs. And $y = x_1$ is the output.

2.6 Parameters identification

2.6.1 Physical identification

The parameters of design of the electromagnetic system are showed in the table 2.1. This parameters were explained in section 2.5.1. The value of this characteristics of the system was directed measured from the prototype model plant in figure 2.1, from the reference in the paper [Sue14] and from an autorregresive parametric model from the current signal 2.6. The parameter μ_0 (the air permeability) is equal to $4\pi \times 10^{-7}$ [Sue14].

Table 2.2: Equivalent parameters in the parametric model.

Parameter	Value	Units
Resistance (R)	1.68	Ω
Inductance (L)	14.87	H

Table 2.1: System physical parameters

Design parameters	Value
N	10
m	0.2 kg
A	$78.537mm^2$
R	2Ω
μ_0	$4\pi \times 10^{-7}$

The resistance and inductance in table 2.1 were obtained from the signal current at the step response of 10.31 volts using an ARMAX model. The step response of the RL circuit model is presented in figure 2.6. The behavior present an overpeak at time 350 [0.35ms]. The model respond to a RLC serial circuit see transfer function 2.37 and 2.38. Finally, considering a RL serial circuit we can obtain the equivalent parameters in the electric circuit (see table 2.2).

$$\frac{i(s)}{V(s)} = \frac{1/L}{s + R/L} \tag{2.37}$$

$$\frac{i(s)}{V(s)} = \frac{0.067247}{s + 0.11274} \tag{2.38}$$

From equation 2.36 replacing all the values from table 2.1 it will obtain the values 2.39,2.40.[1]

$$A = \begin{bmatrix} 0 & 1 & 0 & 0 \\ -2.33 \times 10^6 & 0 & -9.87 \times 10^{-4} & 9.87 \times 10^{-4} \\ -405.31 & 0.2 & -4.05 \times 10^3 & 0 \\ 405.31 & 0.2 & 0 & -4.05 \times 10^3 \end{bmatrix} \tag{2.39}$$

---

[1]The parameters were measured directly from the plant without the power circuit. In chapter 5, it is presented the detailed electric circuit implemented.
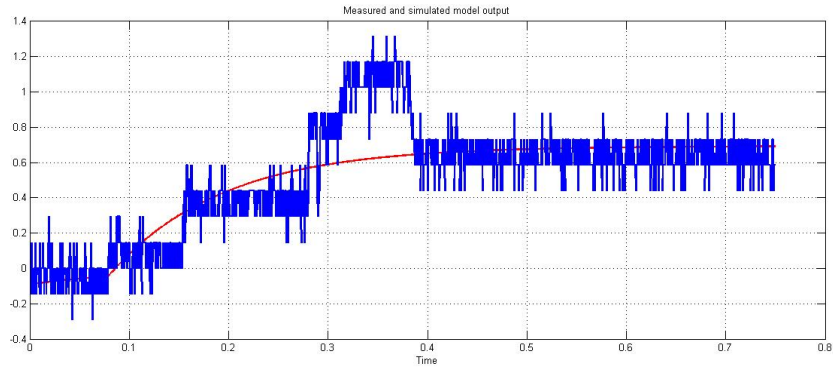
Figure 2.6: Step reponse current at 10.31 Volts and model ARMAX. The measure was achieved by the Allegro ACS712 current sensor.

$$
B = \begin{bmatrix} 0 & 0 \\ 0 & 0 \\ 2.03 \times 10^3 & 0 \\ 0 & 2.03 \times 10^3 \end{bmatrix}
\tag{2.40}
$$
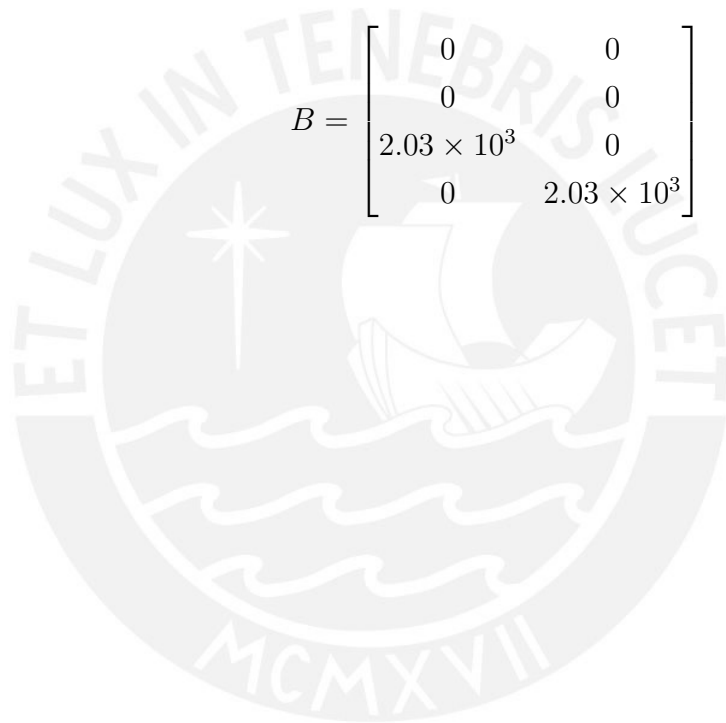
Chapter 3

Control design of the active magnetic bearing system

3.1 Magnetic force

The current and displacement limitations in which the magnetic force can be considered as linear, can be extracted from the surfaces that are presented in the figure 3.1. In this figure, $F_m(x, i_1, i_2) = f_{m1} - f_{m2}$ from equation 2.16 assumes a constant i_2 and varies i_1 from 0 to 8 Amperes.

Figure 3.1: Forces generated in the active magnetic bearing system acoording to $F_m = f_{m1} - f_{m2}$ and i_2 equal to 2, 4, 6 and 8 Amperes.

In order to complete the analysis of the behavior of the magnetic force as linear, it is presented in the figure 3.2 the surfaces of the magnetic force taking constant

Figure 3.2: Forces generated in the active magnetic bearing system acoording to
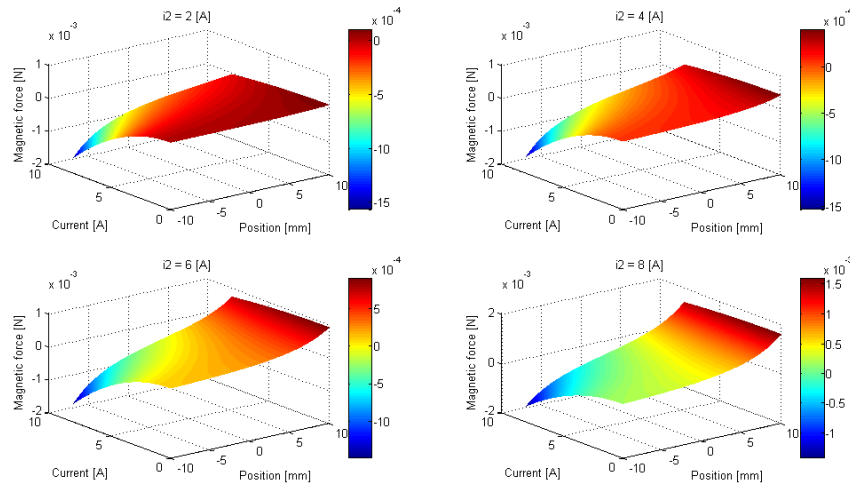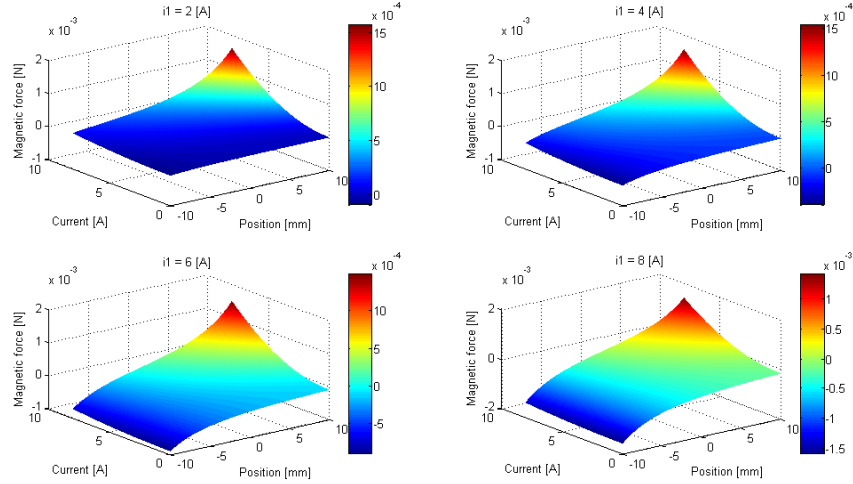$F_m = f_{m1} - f_{m2}$ and i_1 equal to 2, 4, 6 and 8 Amperes.

the current i_1 and varying i_2 from 0 to 8 Amperes.

According to the figures, the behavior of the magnetic force of the system is linear when the position and current values are close to zero. Therefore, it will design the control algorithm with low values for the current and position.

3.2   Optimization problem

Optimization refers to the problem of choosing a set of parameters that maximize or minimize a given function. In control systems, we are often faced with having to choose a set of parameters for a control law so that the some performance condition is satisfied. The next section will seek to optimize a given specification, choosing the parameters that maximize the performance (or minimize the cost J). Consider first the problem of finding the minimum of a smooth function $F : R^n \to R$. That is, we wish to find a point $x^* \in R^n$ such that $F(x^*) \leq F(x)$for all $x \in R^n$. A necessary condition for x^* to be a minimum is that the gradient of the function be zero at x^* as equation 3.1.

$$\frac{\partial F}{\partial x}(x^*) = 0 \tag{3.1}$$

The function $F(x)$ is often called a cost function and x^* is the optimal value for x.

3.2.1   Optimal control of dynamic systems

Consider now $F(x) = J(x, u)$ and the function J is develoved in the equation 3.2. Abstractly, this is a constrained optimization problem where we seek a feasible trajectory (x(t), u(t)) that minimizes the cost function J.

$$F(x, u) = J(x, u) = V(x(T)) + \int_0^T L(x, u)dt \tag{3.2}$$

subject to the constraint 3.3.

$$\dot{x} = f(x, u), x \in R^n, u \in R^m \tag{3.3}$$

More formally, this problem is equivalent to the "standard" problem of minimizing a cost function $J(x, u)$ where $(x, u) \in L_2[0, T]$ (the set of square integrable functions) and $h(z) = \dot{x}(t) - f(x(t), u(t)) = 0$ models the dynamics. The term $L(x, u)$ is referred to as the integral cost and $V(x(T))$ is the final (or terminal) cost. It is important to mention that there are many variations and special cases of the optimal control problem. In the next section it will develop the Linear quadratic (LQ) optimal control considering the infinite horizon optimal control. That is if we let $T = \infty$ and set $V = 0$ in the equation 3.2.

3.3   Control of linear system with quadratic criteria

The active magnetic system developed in equation 2.36 is described by linear dynamic models. Thus, is possible to synthesize very satisfactory linear feedback controllers by the proper choice of quadratic performance criteria and quadratic constraints.

There are differences between terminal controllers and regulators. The terminal controller is designed to bring a system close to the desired conditions at a terminal time while providing acceptable path behavior. A regulator is designed to maintain a stationary system within an acceptable deviation from a reference condition [Bry75]. In this section, optimal algorithm with an integrator is proposed to control the system with quadratic regulator criteria.

3.3.1 Active magnetic bearing linear quadratic regulator

The state-space form in equation 2.36 with the form of the equation 3.4 and the values from equation 2.39 and 2.40.

$$\dot{x}(t) = Ax(t) + Bu(t), y(t) = Cx(t) \tag{3.4}$$

Given x(o), there is a controller is to minimize the cost function expressed in equation 3.5.

$$J(x, u) = \int_0^{+\infty} (x^T Q x + u^T R u) dt \tag{3.5}$$

Where Q and R are positive definite weighting matrices. It is consider to reduce the position parameter so Q will as the equation 3.6.

$$Q = \begin{bmatrix} q_1 & 0 & 0 \\ 0 & 0 & 0 \\ 0 & 0 & 0 \end{bmatrix} \tag{3.6}$$

with $q_1 = 10^6$ and,

$$R = \begin{bmatrix} 1 \end{bmatrix} \tag{3.7}$$

Riccati algorithm (equation 3.9) find a matrix u (equation 3.8) that minimize J the cost function.

$$u = -Kx, K = R^{-1} B^T P \tag{3.8}$$

$$A^T P + P A - P B R^{-1} B^T P + Q = 0 \tag{3.9}$$

Solving the Riccati equation 3.9, it can be solve the value of the maatrix K (see matrix in equation 3.10) in order to obtain the control algorithm.

$$K = \begin{bmatrix} 0.4858 & -8.57 \times 10^{-4} & 2.08 \times 10^{-10} & -2.08 \times 10^{-10} \\ -0.4858 & 8.57 \times 10^{-4} & -2.08 \times 10^{-10} & 2.08 \times 10^{-10} \end{bmatrix} \tag{3.10}$$

In order to regulate the unstable magnetic bearing, it was proposed an optimal control algorithm with and without an integrator structure, which is illustrated in figure 3.3 and for the LQR sistem with an integrator see figure 3.4 and equations 3.11.

$$K_i = \begin{bmatrix} -0.7758 & -0.0014 & 2.48 \times 10^{-10} & 2.48 \times 10^{-10} & -0.0017 \\ 0.7758 & 0.0014 & -2.48 \times 10^{-10} & -2.48 \times 10^{-10} & 0.0017 \end{bmatrix} \tag{3.11}$$
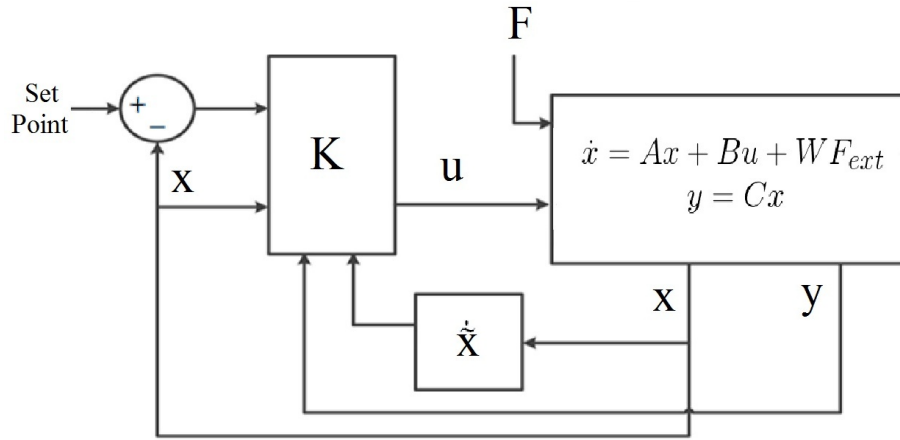
Figure 3.3: Diagram block without an integrator of the complete system
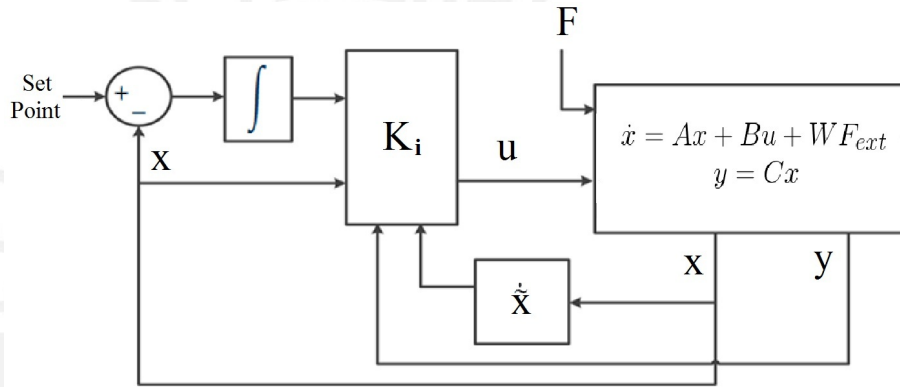
Figure 3.4: Diagram block with an integrator of the complete system

The optimal value of cost function is obtained by equation 3.12.

$$J = x^T(0)Px(0) \tag{3.12}$$

The optimal value of cost function depends on the initial condition of $x(t = 0) = x(0)$.

Stability can be proven by considering the Lyapunov function. From closed loop system state equation can be provided by equation 3.13.

$$\dot{x} = (A - BR^{-1}B^T P)x \tag{3.13}$$

The Lyapunov function is expressed by equation 3.14.

$$V = x^T Px \tag{3.14}$$

Using the Riccati equation 3.9, the Lyapunov derivative is given by equation 3.15 and 3.16.

$$\dot{V}(x) = -x^T(PBR^{-1}B^TP)x - x^TQx, \dot{V}(x) < 0 \qquad (3.15)$$

$$\dot{V}(x) < 0 \qquad (3.16)$$

Since the Lyapunov derivative is negative, it concludes that closed loop control system is stable.

3.4 Optimal linear preview control of active magnetic bearing

The optimal linear preview control formulation of the problem is as follows. Consider the system in the equation (3.17).

$$\dot{x}(t) = Ax(t) + Bu(t) + W_r r, x(t_0) = x_0 \qquad (3.17)$$

Where A, B and W_r are $(n \times n)$, $(n \times m)$ and $(r \times n)$ matrices, respectively. $x(t) \in R^n, u(t) \in R^m$ and $r(t) \in R^q$ are the state, control input, and disturbance vectors, respectively. Furthermore, x_0 is a stochastic vector with mean $\bar{x}_0$ and variance S_0, $r(t)$ is a random vector with zero mean and unknown second order statistics.

The cost function is (3.18)

$$J = \int_t^\infty (\frac{1}{2}x^TQx + \frac{1}{2}u^TRu)dt \qquad (3.18)$$

$$J = \int_t^{t+t_p} (\frac{1}{2}x^TQx + \frac{1}{2}u^TRu)dt + \int_{t+t_p}^\infty (\frac{1}{2}x^TQx + \frac{1}{2}u^TRu)dt \qquad (3.19)$$

$$J = \int_t^{t+t_p} (\frac{1}{2}x^TQx + \frac{1}{2}u^TRu)dt + \frac{1}{2}x_{(t+tp)}^T \bar{P}x_{(t+t_p)} \qquad (3.20)$$

Then, Lagrange function for the cost function (3.20) considering the sistem (3.17) is as follows in (3.21).

$$L(x,u) = \frac{1}{2}x_{(t+tp)}^T \bar{P}x_{(t+t_p)} + \int_t^{t+t_p} (\frac{1}{2}x^TQx + \frac{1}{2}u^TRu)dt + \int_t^{t+t_p} \lambda^T(Ax + Bu + W_r - \dot{x})dt \qquad (3.21)$$

So, the Hamiltonian is (3.22).

$$H = \frac{1}{2}x^TQx + \frac{1}{2}u^TRu + \lambda^T(Ax + Bu + W_r - \dot{x}) \qquad (3.22)$$

Solving the equation (3.23). It obtain the two point boundary value in equation (3.24) and (3.25).

$$\frac{dL(x,u)}{dx} = 0 \tag{3.23}$$

$$\dot{\lambda} = -\frac{dH}{dx} \tag{3.24}$$

$$\lambda = \frac{\partial}{\partial x_{(t+t_p)}}(\frac{1}{2}x_{(t+tp)}^T \bar{P}x_{(t+t_p)}) \tag{3.25}$$

Then, solving the equation (3.24) and (3.27). It obtain the equation (3.26) and (3.28).

$$\dot{\lambda} = -Qx - A^T\lambda \tag{3.26}$$

$$\frac{dL(x,u)}{du} = 0 \tag{3.27}$$

$$u = -R^{-1}B^T\lambda \tag{3.28}$$

It is consider that λ is equivalent by two components as follow in equation (3.29).

$$\lambda = Px + q \tag{3.29}$$

From (3.17), (3.28), (3.17), (3.17) and (3.29) it obtain the following equation (3.30).

$$(\dot{P}+A^TP+PA-PBR^{-1}B^TP+Q)x+(\dot{q}+(A^T-PBR^{-1}B^T)q+PW_rr) = 0 \tag{3.30}$$

In (3.30), where P is considered constant and it is obtained solving the Riccati equation in 3.31.

$$A^TP + PA - PBR^{-1}B^TP + Q = 0 \tag{3.31}$$

Then, solving the equation 3.32 from 3.30 it obtain the relation in 3.33 with $A_{CL}^T = A^T - PBR^{-1}B^T$ and 3.34.

$$\dot{q} + (A^T - PBR^{-1}B^T)q + PW_rr = 0 \tag{3.32}$$

$$\dot{q} = -A_{CL}^Tq - PW_rr \tag{3.33}$$

$$q = \int_0^{t_p} e^{A_{CL}^T\beta}PW_rr_{(t+\beta)}d\beta \tag{3.34}$$

For porpuses of simulating the control algorithm, the equation in 3.34 is represented

as 3.35

$$q = \sum_{n=0}^{n\Delta t = t_p} e^{A_{CL}^T n \Delta t} P W_r r_{(k+n)} \Delta t \tag{3.35}$$

Finally, the u that minisize the cost function is $u = -R^{-1}B^T(Px + q)$ (see equation 3.36 and 3.37).

$$u = -R^{-1}B^T P x - R^{-1}B^T \int_0^{t_p} e^{A_{CL}^T \beta} P W_r r_{(t+\beta)} d\beta) \tag{3.36}$$

$$u_{(k)} = -R^{-1}B^T P x_{(k)} - R^{-1}B^T \sum_{n=0}^{n\Delta t = t_p} e^{A_{CL}^T n \Delta t} P W_r r_{(k+n)} \Delta t \tag{3.37}$$

Chapter 4

Simulation and results of the active magnetic bearing system

In this chapter, it is presented the simulation and results of the algorithms proposed in the active magnetic bearing model developed in chapter 3. The simulations consider a input force in the system. The force represents the vibrational movement of the motor.

4.1 Linear quadratic regulator

4.1.1 Linear quadratic regulator without an integrator system

Acoording to the LQR control, the active magnetic bearing is controllable. Riccati algorithm show that the ecuations are stable (see figure 4.1).

4.1.2 Linear quadratic regulator with an integrator system

Another simulations results of the controller design in the active magnetic system adding an integrator to the control algorithm linear quadratic regulator. The control simulation are illustrated in the figures 4.2, 4.3. Figure 4.2 shows the control of the nonlinear system with the control algorithm with integrator. The system is initially out of phase in $z_0 = 0$ millimeters. In addition, to simulate the vibration of the engine. The sinusoidal force F is simulated as external to the system. In figure 4.2, the current of an electric system i_1 is shown. The other current i_2 has the similar behavior.
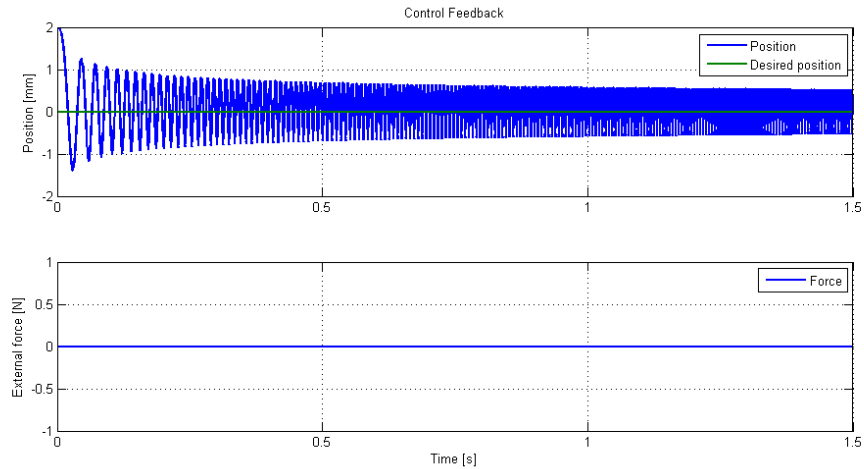
Figure 4.1: Simulation of the mathematical plant with optimal control feedback.

This kind of control have better performance than linear quadratic regulator (LQR) system without an integrator.

Figure 4.3 shows the control of the nonlinear system with the control algorithm with integrator. However, the system is initially out of phase in $z_2 = 2$ millimeters. The sinusoidal force F is simulated as external to the system.

Figure 4.2: Simulation of the mathematical plant with optimal linear quadratic regulator control feedback with an integrator in the system. The input in this simulation is an external force $F = Asin(wt)[N]$ with $A = 30$, $w = 20rad/s$, initial value $z_0 = 0mm$ and time t in seconds.
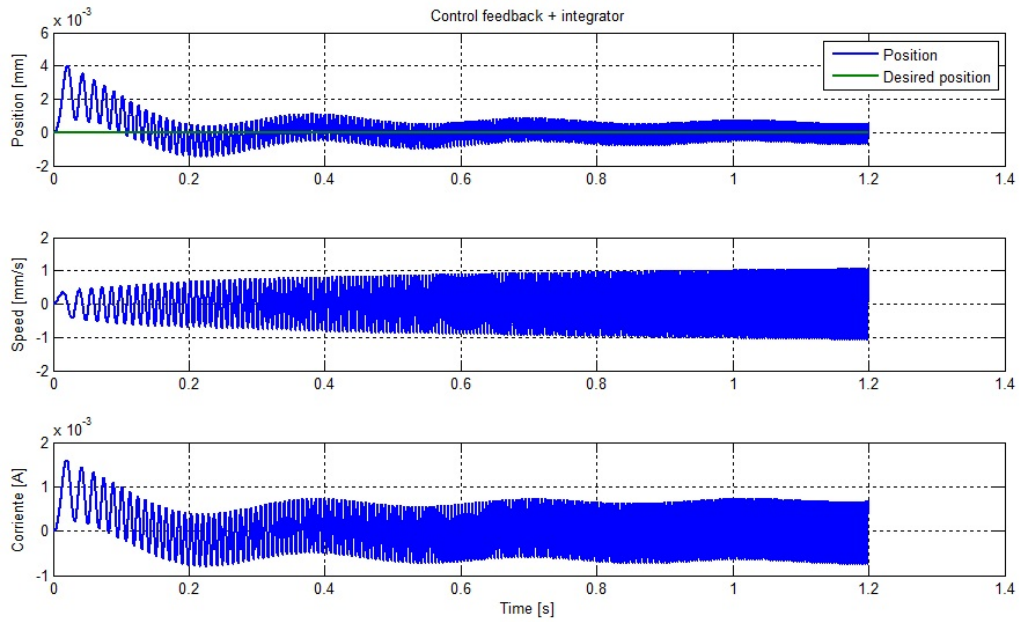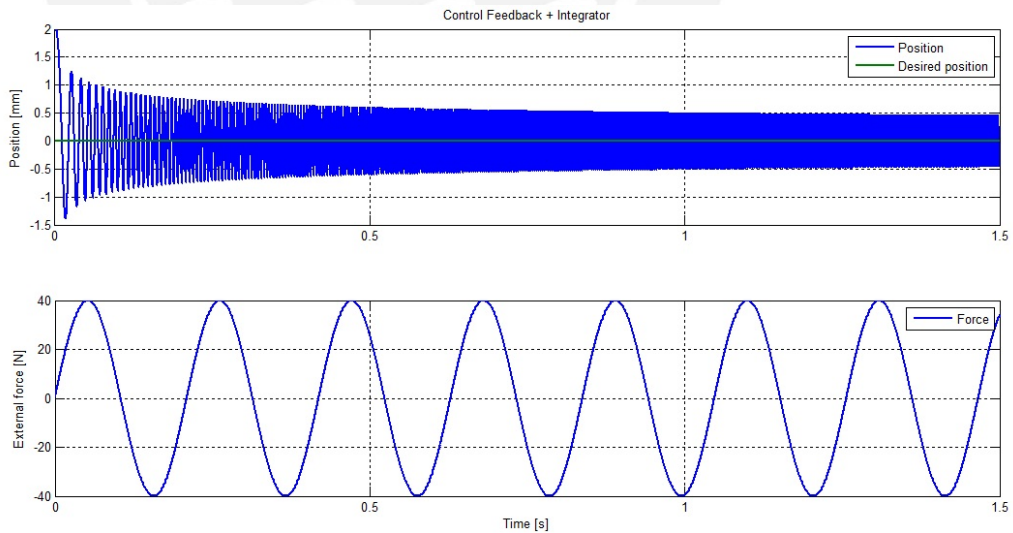

Figure 4.3: Simulation of the mathematical plant with optimal linear quadratic regulator control feedback with an integrator in the system. The input in this simulation is an external force $F = Asin(wt)[N]$ with $A = 40$, $w = 30rad/s$, initial value $z_0 = 2mm$ and time t in seconds.

51

Chapter 5

Experimental tests of the active magnetic bearing prototype

In this chapter, it is presented the experimental results for the control algorithm proposed. In addition, it is detailed the position sensor, real time control and the electronic circuit.

5.1   Active magnetic bearing prototype

The parts of the final prototype are presented in the figure 5.1.[1]

---

[1]The prototype was designed by Alan Calderón, also it was improved by Danilo Aragón and Carlos Perea in order to optimize its data system identification with its controller.
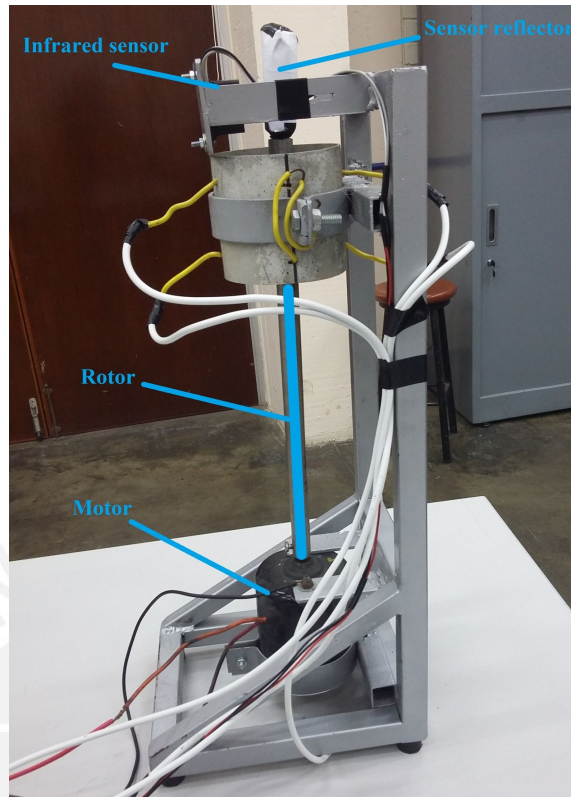
Figure 5.1: Parts of the Active Magnetic Bearing Prototype

In order to control the mechatronic system, it was implemented the electronic system to control one axis as it is showed in figure 5.2.
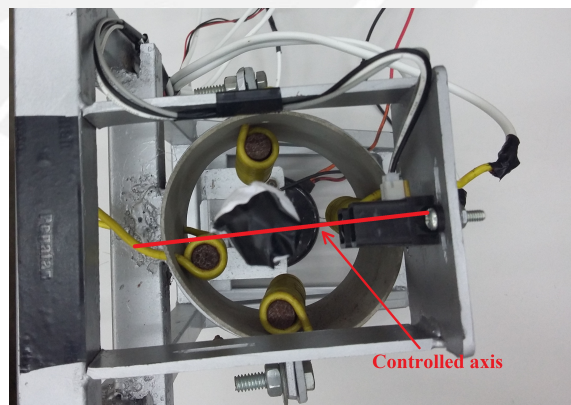

Figure 5.2: Active Magnetic Bearing Prototype controlled axis.

5.1.1   Electric parameters identification

Considering the electronic power (BTJs transistor) there are power losses that were identificated by a ARMAX model. The voltage power losses in the BJTs transistor

are 0.845 Volts. Thus, the maximun voltage supply has to reduce in 1.69 Volts. Second, there were identificated the capacitor and resistance value of the total bridge H implemented.

5.2   Distance sensor

5.2.1   Angular velocity

General purpose type distance measuring sensor GP2Y0A21YK was tested.

In figure 5.3, the infrared sensor measures the position of the rotor when the system is not controlled.

The spectral frequency of the signal is showed in the figure 5.4. In this figure there is a peak of the frequency identified by the spectral data in frequency 8 hertz.

The angular frequency of the motor is the same as the frequency of the rotor. The frequency of rotor rotation is obtained because of its frequency analysis. To obtain the signal of the sensor with less white noise, the Kalman filter was used.
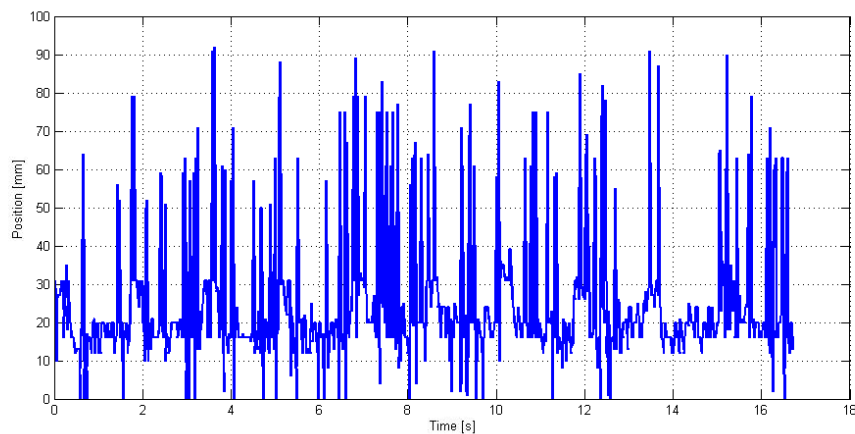

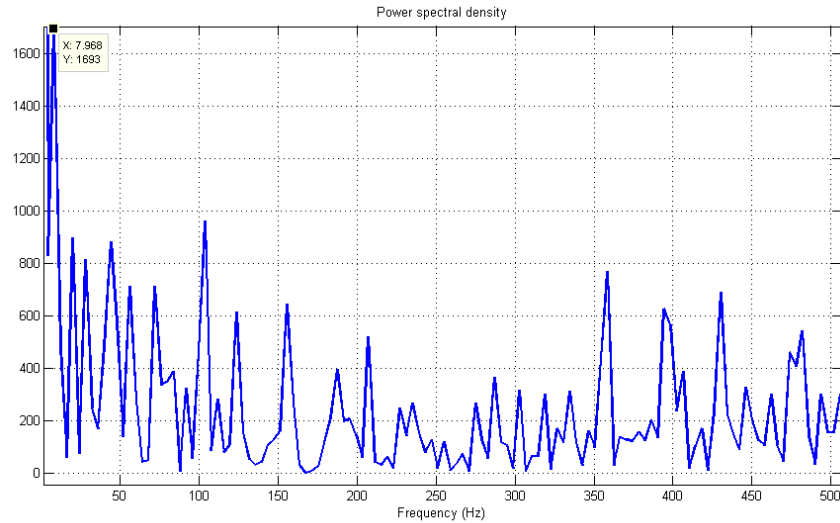Figure 5.3: Direct measured position of the rotor displacement.

54

Figure 5.4: Spectral frecuency from the test analysis of the position of the rotor.

5.2.2 Kalman filter for gaussian noise

There is the signal measured with the motor on in low velocity (see figure 5.5). The statistical kalman filter is applied with different types of variance tested on the sensor (see figure 5.6). From estimation of the sensor variance, the infrared sensor for two centimeters of distance is approximately 100. That is the second filter in the figure 5.6. The Kalman filter assumes that the measure of the sensor has additive white gaussian noise. Then, the signal is cleaned by an estimator and it is obtained the measure of the sensor.
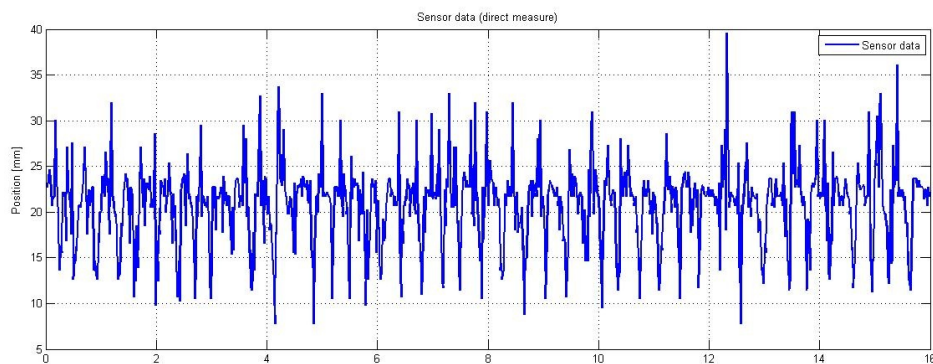

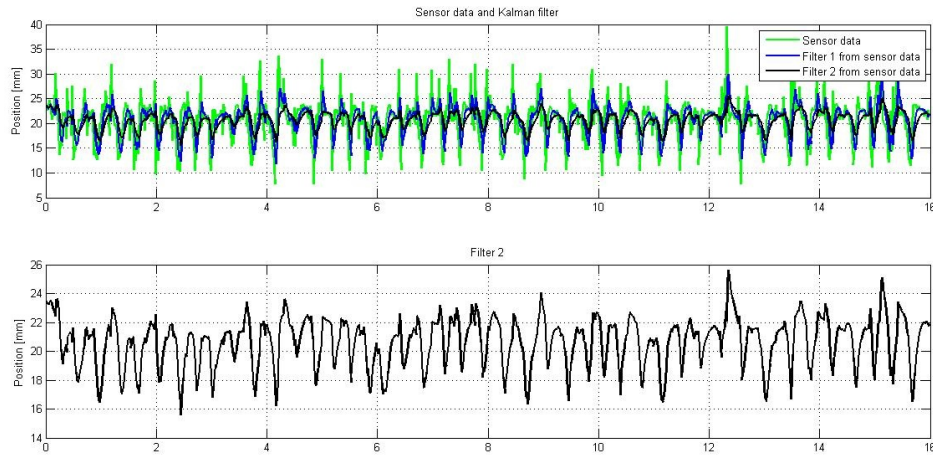Figure 5.5: Direct measure to the rotor in the AMB from infrared sensor when the motor is on

Tesis publicada con autorización del autor
No olvide citar esta tesis

Figure 5.6: Direct measure and filter by Kalman theory with two diferents variance asumming white gaussian noise in the data sensor

5.3 Multi Tasking in Small Embedded Systems

In more recent times processing power has become less expensive so each user can have exclusive access to one or more processors. The scheduling algorithms in these types of system are designed to allow users to run multiple applications simultaneously without the computer becoming unresponsive. The control algorithm for an Active magnetic bearing has several task to achieve in parallel programing. It is proposed to use the FreeRTOS real time kernel [Bar10]. In this case the ATmega 338P is employed in order to achieve the real time control.

5.3.1 The FreeRTOS Family

FreeRTOS uses a modified GPL license. The modification is included to ensure: 1. FreeRTOS can be used in commercial applications. 2. FreeRTOS itself remains open source. 3. FreeRTOS users retain ownership of their intellectual property.

When you link FreeRTOS into an application, you are obliged to open source only the kernel, including any additions or modifications you may have made. Components that merely use FreeRTOS through its published API can remain closed source and proprietary.

OpenRTOS Shares the same code base as FreeRTOS, but is provided under standard commercial license terms. The commercial license removes the requirement to open source any code at all and provides IP infringement protection. OpenR-

TOS can be purchased with a professional support contract and a selection of other useful components such as TCP/IP stacks and drivers, USB stacks and drivers, and various different file systems. Evaluation versions can be downloaded from http://www.OpenRTOS.com. Table 5.1 provides an overview of the differences between the FreeRTOS and OpenRTOS license models.

Table 5.1: Comparing the FreeRTOS license with the OpenRTOS license [Bar10].

	FreeRTOS License	OpenRTOS License
Is it Free?	Yes	No
Can I use it in a commercial application?	Yes	Yes
Is it royalty free?	Yes	Yes
Do I have to open source my application code that makes use of FreeRTOS services?	No, as long as the code provides functionality that is distinct from that provided by FreeRTOS	No
Do I have to open source my changes to the kernel?	Yes	No
Do I have to document that my product uses FreeRTOS?	Yes	No
Do I have to offer to provide the FreeRTOS code to users of my application?	Yes	No
Can I buy an annual support contract?	No	Yes
Is a warranty provided?	No	Yes
Is legal protection provided?	No	Yes

5.3.2 Flowchart for the control algorithm

The Real time controller program of the system is adapted to the design conditions in chapter 3. The algorithm for the control is ejecuted in a threat every 500 micro seconds (see figure 5.7). The control of the voltage was achieved by using a PWM system and a bridge H for negative voltage in order to control the current in the magnetic subsystem. The flowchart for the control of the voltage is presented in the figure 5.8.
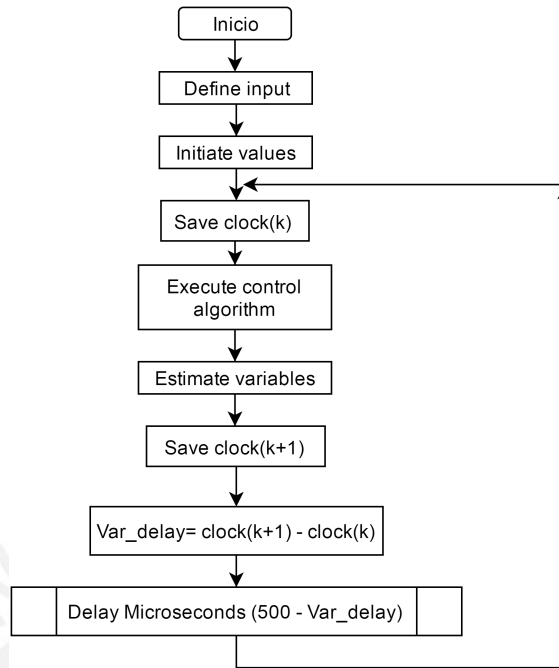
Figure 5.7: Flowchart for the control algorithm thread. Note that it has to execute every 500 micro seconds to achieve the algorithm.
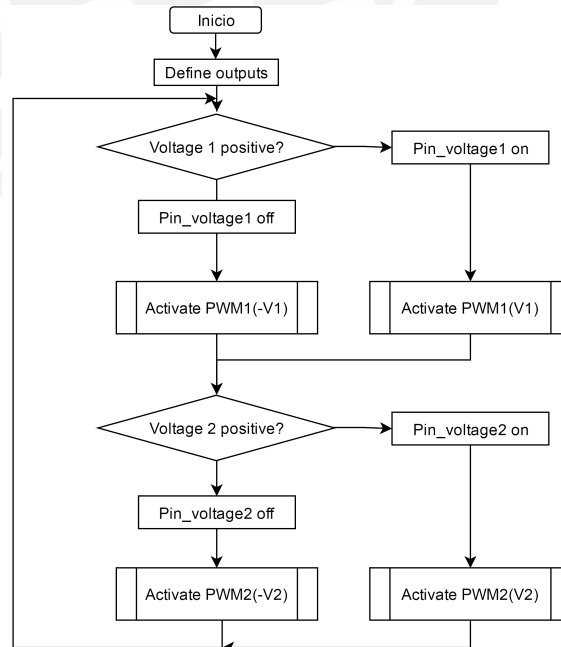

Figure 5.8: Flowchart for the voltage control with PWM signal and with positive and negative values in order to achieve the control in the current.

5.4   Electronic circuit

To explain the electronic circuit, the present section will show electronics in three parts: potencial circuit, logic gates and electronic conditioning and controller.

5.4.1   Potencial circuit

Two bridges H were developed in order to control one axis (see figures 5.9 and 5.10). There were used Darlington Power Transistors (TIP142 and TIP147). The system can support 10 amperes and 100 Volts.
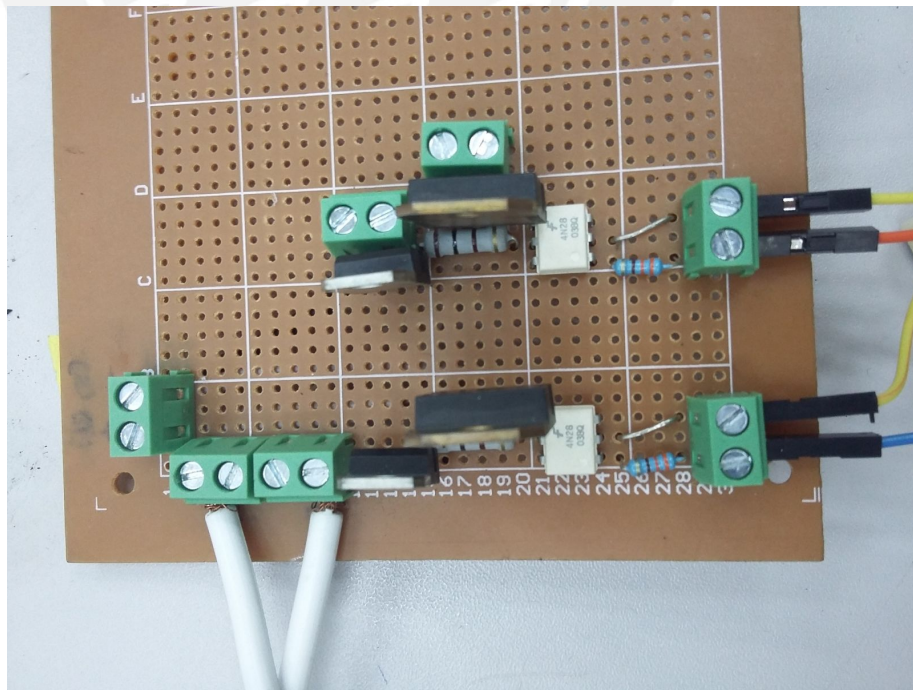

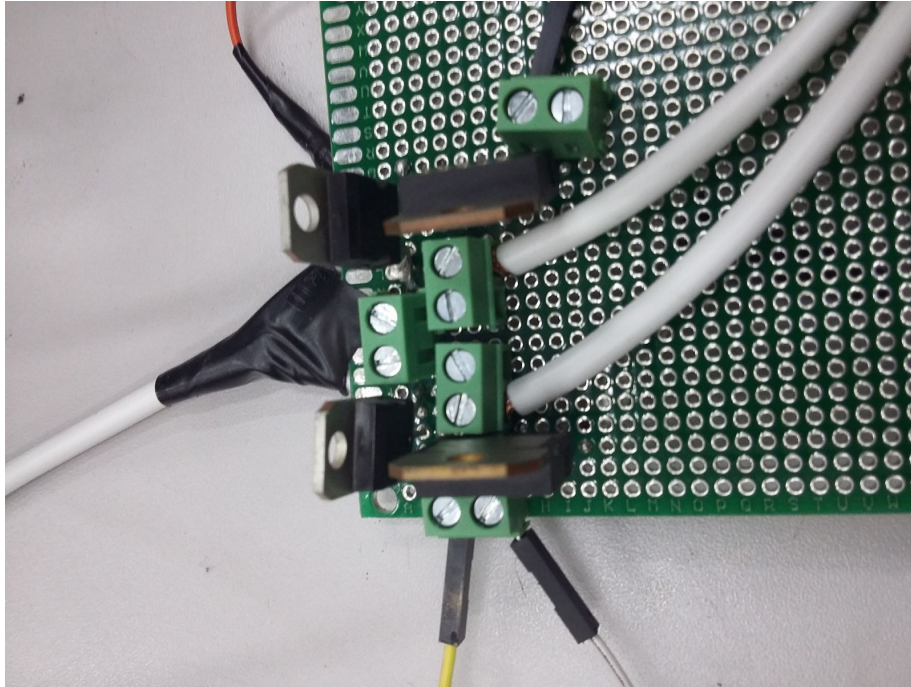Figure 5.9: First bridge H to control one coil.

Figure 5.10: Second bridge H to control the opposite coil.

5.4.2 Logic gates

The real-time program becomes more difficult to perform and it would require 4 outputs PWM Arduino if it were not for the implemented logic gates. In addition, it ensures that the source doesn't do short-circuit, since this state is prohibited. In order to reduce the control variables, it is proposed the following logic gates in the power subsystem (see figure 5.11 and figure 5.12). Note that the true and true logic output is prohibited.. The PWM signal has no problem in order to simulate voltage positive and negative values with the logic gates.
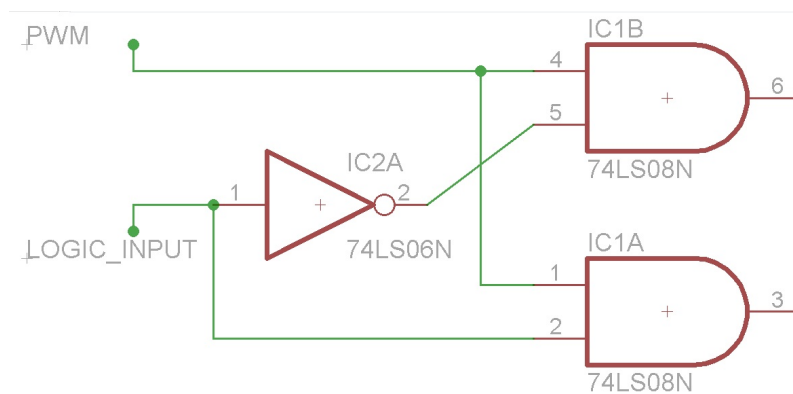
Figure 5.11: Logic circuit schematic.
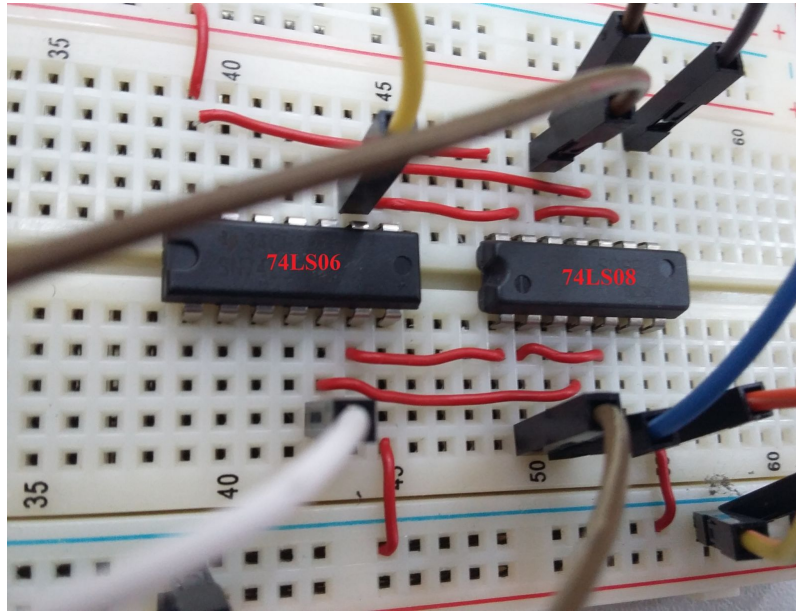
Figure 5.12: Logic circuit conections. The prototype logic circuit was implemented in a protoboard.

5.4.3 Electronic conditioning and controller

The sensor conditioning and bridge H conditioning is presented in this subsection. There were used Arduino Uno in the implementation (see figure 5.13).

Figure 5.13: Electronic conditioning and controller schematic.

5.5 Experimental control tests

The infrared sensor achieved position measured by using an estimator in the control algorithm. Outside the control algorithm the infrared sensor measured angular

velocity by using a Kalman filter and analyzing the spectral frequency.

The measure value without a filter is presented in the figure 5.14. Note that there are high peaks because the of the particular noise in the infrared sensor. The data were analized an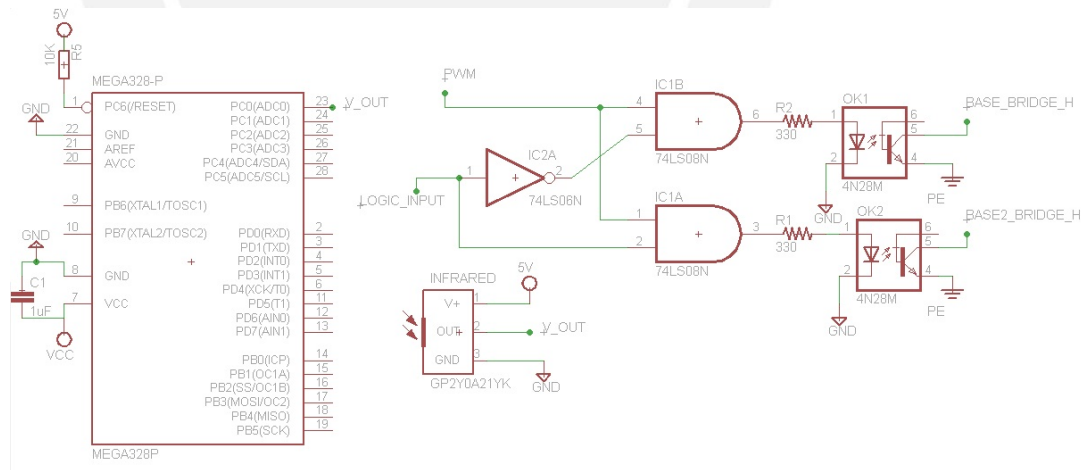d it was applied a low pass filter in order to filter this frequencies (see figure 5.15). In this figure, there are the values from the infrared sensor that are visible to interpret. The maximum amplitude measure is clearly 12 mm.
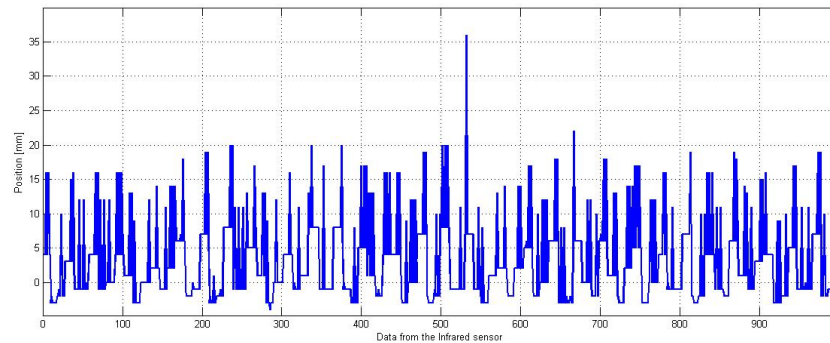
Figure 5.14: Position uncontrolled system without filter.

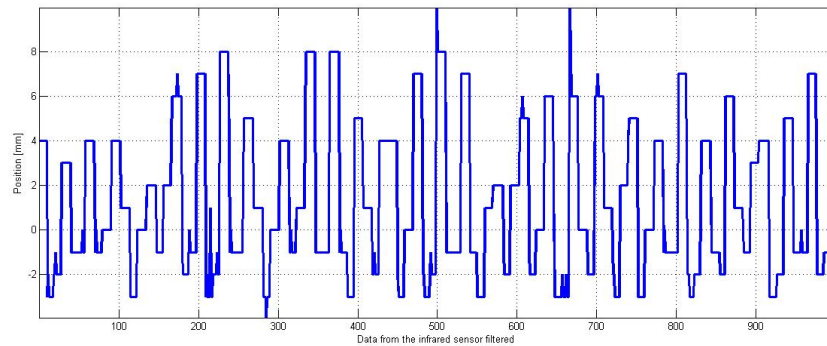Figure 5.15: Position uncontrolled system with low pass filter.

The algorithm control considering all the implementation and the motor at 2600 RPM is sensed and presented in the figure 5.16. The algorithm in this case is the optimal control with an integrator. The amplitud is controlled. The maximum amplitude is 6 mm aproximately. The frequency range is proved in 2600 RPM or more for the prototype.
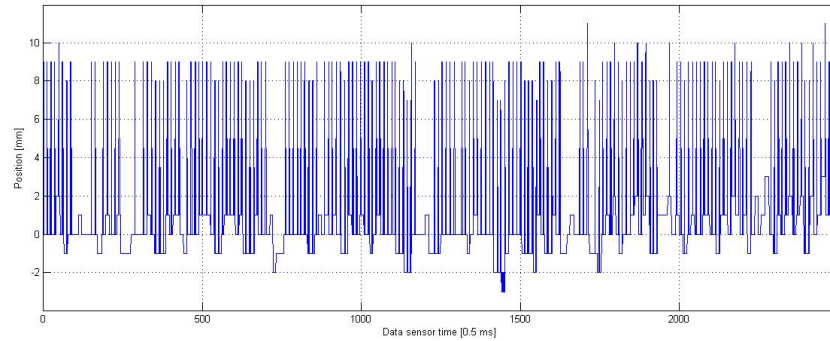
Figure 5.16: Position controlled system without filter.

The filtered signal is presented in the figure 5.17. The amplitude is finally reduced to 7 mm aproximately. The high peaks of the infrared sensor are the unfiltered sensor data. This is the behavior of the sensor for measurements between 0 to 100 mm. The real-time control estimator cleans the signal by taking Gaussian white noise and the physical equations of the system as data. In the figures, it is possible to compare the system without control and the controlled system.
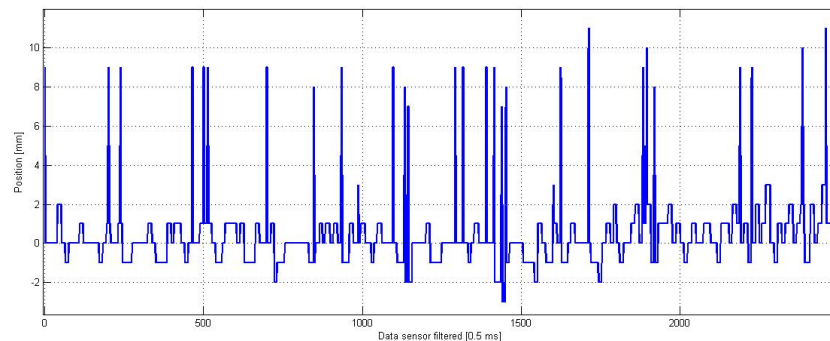
Figure 5.17: Position controlled system filtered.

5.6   Discussion of results

- It is necesary to achieve a correctly identification in order to control the current in the electric subsystem.

- It is recommendable reduce the capacitance in the power circuit because the capacitance reduces the maximum force in the electromagnets.

- It was suggested to use the magnetic bearing modeling by a mathematical model in this thesis. However, the prototype more detailed modeling is developed in

another thesis.

Chapter 6

Conclusions

- Real time control was implemented in this thesis succesfully.

- The system behavior with the implemented control reports high instability at low frequencies.

- High frequencies in the motor present better results in the control implemented.

- The state space algorithm of the system was achieved in the chapter 2.

- The autoregressive model obtain the electric parameters.

- Two linear quadratic regulated (LQR) controllers were presented in this thesis.

- It was implemented an estimator inside all the control algorithms presented.

- In the real time program, the estimator filter the noise from the position sensor.

6.1   Future work

- The prototype design has a bearing support. This is mostly a theoretical case, in practice most applications have two supports. Normally, two magnetic bearings are used in a floating rotor. Therefore, it is suggested to work with floating rotor in a vertical way, since the gravity would alter the equilibrium points that were explained in this thesis.

- It is possible to achieve a more precisely control taking a better controller and all the physics equations such as the capacitor component in the power circuit system. The system would be evaluated at the input step (see figure 6.1). Note that the behavior present an overpeak at time 350 [0.35ms]. Therefore, the

circuit model is considered of second order. The step reponse in the stimated autoregresive modeling is showed in the figure 6.2. The model respond to a RLC serial circuit see transfer function 6.1. The overpeak in the model 6.2 correspond succesfully with the figure 6.1. Finally, considering a RLC serial circuit we can obtain the equivalent parameters in the electric circuit (see table 6.1). It is consider a RLC serial circuit because the step response in the current presented an overpeak.

$$\frac{i(s)}{V(s)} = \frac{sC}{LCs^2 + RCs + 1}$$ (6.1)
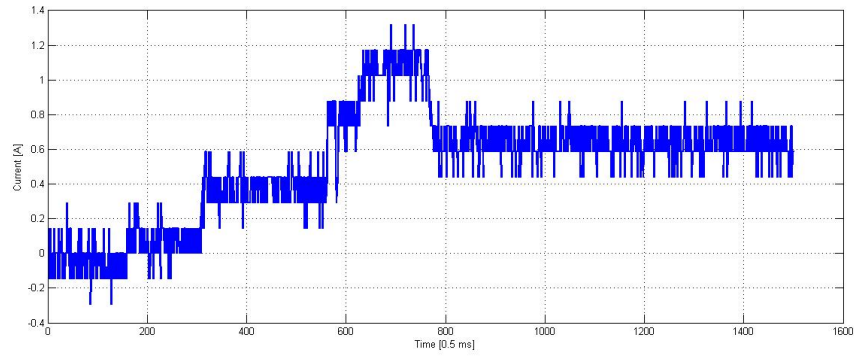

Figure 6.1: Step reponse current at 10.31 volts. The measure was achieved by the Allegro ACS712 current sensor.
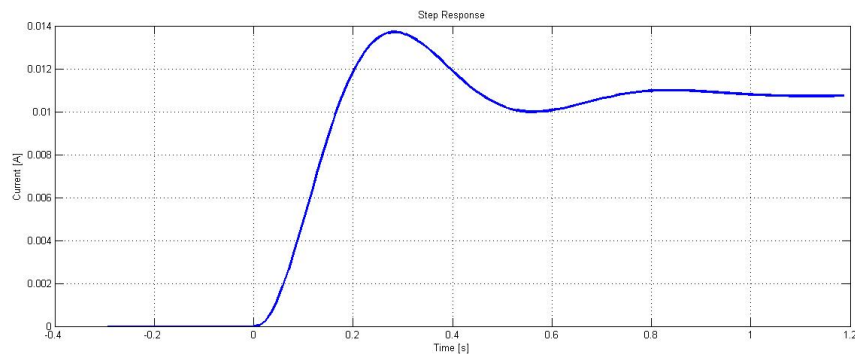

Figure 6.2: The model step reponse current at 1 volts.

66

Table 6.1: Equivalent parameters in the parametric model.

Parameter	Value	Units
Resistance (R)	5.81	Ω
Inductance (L)	0.618	H
Capacitance (C)	10.786	mF

Bibliography

[AO10]   Roger Achkar and Michel Owayjan. Control of an active magnetic bearing with multi-layer perceptrons using the torque method. In *Intelligent Systems Design and Applications (ISDA), 2010 10th International Conference on*, pages 214–219. IEEE, 2010.

[Bar10]   Richard Barry. *Using the FreeRTOS real time kernel: a practical guide.* Real Time Engineers, 2010.

[BCK+09]   Hannes Bleuler, Matthew Cole, Patrick Keogh, R Larsonneur, E Maslen, Y Okada, G Schweitzer, A Traxler, Gerhard Schweitzer, Eric H Maslen, et al. *Magnetic bearings: theory, design, and application to rotating machinery.* Springer Science & Business Media, 2009.

[Bet00]   Felix Betschon. *Design principles of integrated magnetic bearings.* PhD thesis, Diss. Technische Wissenschaften ETH Zürich, Nr. 13643, 2000, 2000.

[BH97]   P Berkelman and R Hollis. Magnetic levitation haptic interfaces will impact training and design. *SPIE OE Reports*, (165), 1997.

[BHP12]   Kevin D Bachovchin, James F Hoburg, and Richard F Post. Magnetic fields and forces in permanent magnet levitated bearings. *Magnetics, IEEE Transactions on*, 48(7):2112–2120, 2012.

[BHP13]   Kevin D Bachovchin, James F Hoburg, and Richard F Post. Stable levitation of a passive magnetic bearing. *Magnetics, IEEE Transactions on*, 49(1):609–617, 2013.

[Bic91]   J Bichsel. The bearingless electrical machine. In *International Symposium on Magnetic Suspension Technology*, volume 2, pages 1–14. Citeseer, 1991.

[Ble92] Hannes Bleuler. A survey of magnetic levitation and magnetic bearing types. *JSME international journal. Ser. 3, Vibration, control engineering, engineering for industry*, 35(3):335–342, 1992.

[Bry75] Arthur Earl Bryson. *Applied optimal control: optimization, estimation and control.* CRC Press, 1975.

[BZW12] JG Bai, XZ Zhang, and LM Wang. A flywheel energy storage system with active magnetic bearings. *Energy Procedia*, 16:1124–1128, 2012.

[CAP+16] Jesús A Calderón, Danilo E Aragón, Carlos A Perea, Oscar Melgarejo, Julio C Tafur, and Benajamín Barriga. Control strategies for a prototype of active magnetic bearing system. In *Cybernetics, Robotics and Control (CRC), International Conference on*, pages 22–26. IEEE, 2016.

[CJM04] Daniel J Clark, Mark J Jansen, and Gerald T Montague. An overview of magnetic bearing technology for gas turbine engines. *National Aeronautics and Space Administration*, 2004.

[FM01] Alexei V Filatov and Eric H Maslen. Passive magnetic bearing for flywheel energy storage systems. *Magnetics, IEEE Transactions on*, 37(6):3913–3924, 2001.

[G+10] Erik Gregersen et al. *The Britannica Guide to Electricity and Magnetism.* Britannica Educational Publishing, 2010.

[Gem97] Thomas Gempp. *Mechatronik einer lagerlosen Spaltrohrpumpe.* PhD thesis, Diss. Techn. Wiss. ETH Zürich, Nr. 12325, 1997. Ref.: J. Hugel; Korref.: G. Schweitzer, 1997.

[GKTK11] T Glück, W Kemmetmüller, C Tump, and A Kugi. A novel robust position estimator for self-sensing magnetic levitation systems based on least squares identification. *Control Engineering Practice*, 19(2):146–157, 2011.

[HS+91] Ralph L Hollis, Septimiu E Salcudean, et al. A six-degree-of-freedom magnetically levitated variable compliance fine-motion wrist: design, modeling, and control. *Robotics and Automation, IEEE Transactions on*, 7(3):320–332, 1991.

[HZLX13] Bangcheng Han, Shiqiang Zheng, Yun Le, and Sheng Xu. Modeling and analysis of coupling performance between passive magnetic bearing and hybrid magnetic radial bearing for magnetically suspended flywheel. *Magnetics, IEEE Transactions on*, 49(10):5356–5370, 2013.

[Jay81] Bhalchandra Vinayak Jayawant. *Electromagnetic levitation and suspension techniques*. 1981.

[Jay88] BV Jayawant. Review lecture. electromagnetic suspension and levitation techniques. In *Proceedings of the Royal Society of London A: Mathematical, Physical and Engineering Sciences*, volume 416, pages 245–320. The Royal Society, 1988.

[JJYX09] Fang Jiancheng, Sun Jinji, Xu Yanliang, and Wang Xi. A new structure for permanent-magnet-biased axial hybrid magnetic bearings. *Magnetics, IEEE Transactions on*, 45(12):5319–5325, 2009.

[Kan03] MS Kang. Optimal feedforward control of active magnetic bearing system subject to base motion. In *Control Applications, 2003. CCA 2003. Proceedings of 2003 IEEE Conference on*, volume 1, pages 748–753. IEEE, 2003.

[KBN07] Boris M Klebanov, David M Barlam, and Frederic E Nystrom. *Machine elements: life and design*. CRC Press, 2007.

[KNN06] P Kummeth, W Nick, and HW Neumüller. Development of superconducting bearings for industrial application. In *Proc. 10th Internat. Symp. on Magnetic Bearings, page Keynote, Martigny, Switzerland*, 2006.

[KSI14] SH Kim, Jae Won Shin, and Kazushi Ishiyama. Magnetic bearings and synchronous magnetic axial coupling for the enhancement of the driving performance of magnetic wireless pumps. *Magnetics, IEEE Transactions on*, 50(1):1–4, 2014.

[LDD+14] Xianxing Liu, Jinyue Dong, Yi Du, Kai Shi, and Lihong Mo. Design and static performance analysis of a novel axial hybrid magnetic bearing. *Magnetics, IEEE Transactions on*, 50(11):1–4, 2014.

[Lev15] Levitec. Levitec company, 2015. [Accessed: 05-10-2015].

[LJKA06] Ki-Chang Lee, Yeon-Ho Jeong, Dae-Hyun Koo, and Hyeong Joon Ahn. Development of a radial active magnetic bearing for high speed turbomachinery motors. In *SICE-ICASE, 2006. International Joint Conference*, pages 1543–1548. IEEE, 2006.

[M$^+$92] Robert L Mott et al. *Machine Elements In Mechanical Design by Robert L Mott: Machine Elements In Mechanical Design*. Digital Designs, 1992.

[MEC15] MECOS. Mecos company, 2015. [Accessed: 04-10-2015].

[MYJF05] Zong Ming, Liu Yuhang, Shen Jixiu, and Wang Fengxiang. Force analysis for hybrid radial magnetic bearing biased by permanent magnet. In *Electrical Machines and Systems, 2005. ICEMS 2005. Proceedings of the Eighth International Conference on*, volume 3, pages 1834–1837. IEEE, 2005.

[PKM$^+$01] MA Pichot, JP Kajs, BR Murphy, A Ouroua, BM Rech, RJ Hayes, JH Beno, GD Buckner, and AB Palazzolo. Active magnetic bearings for energy storage systems for combat vehicles. *Magnetics, IEEE Transactions on*, 37(1):318–323, 2001.

[PMB] Passive magnetic bearings. http://www.magneticbearings.org/technology-2/technologies/passive-bearings/. Accessed: 2015-11-15.

[SGLY06] Yu Suyuan, Yang Guojun, Shi Lei, and XU Yang. Application and research of the active magnetic bearing in the nuclear power plant of high temperature reactor. In *Proceedings of the 10th International Symposium on Magnetic Bearings*, 2006.

[SH08] Pranab Samanta and Harish Hirani. Magnetic bearing configurations: Theoretical and experimental studies. *Magnetics, IEEE Transactions on*, 44(2):292–300, 2008.

[Sin87] Pradip K Sinha. Electromagnetic suspension dynamics & control. 1987.

[SKF] Rolling bearings. http://www.skf.com/binary/56-121486/SKF-rolling-bearings-catalogue.pdf. Accessed: 2015-11-18.

[Sli] Sliding bearings. http://www.ntn.co.jp/english/products/plainbearing.html. Accessed: 2015-11-15.

[SMS03] JA Santisteban, SRA Mendes, and DS Sacramento. A fuzzy controller for an axial magnetic bearing. In *Industrial Electronics, 2003. ISIE'03. 2003 IEEE International Symposium on*, volume 2, pages 991–994. IEEE, 2003.

[SP04] Pradip K Sinha and Alexandre N Pechev. Nonlinear h∞ controllers for electromagnetic suspension systems. *IEEE Transactions on Automatic Control*, 49(4):563–568, 2004.

[Sue14] Anan Suebsomran. Optimal control of electromagnetic suspension ems system. *The Open Automation and Control Systems Journal*, 6(1), 2014.

[SWH95] Septimiu E Salcudean, NM Wong, and Ralph L Hollis. Design and control of a force-reflecting teleoperation system with magnetically levitated master and wrist. *Robotics and Automation, IEEE Transactions on*, 11(6):844–858, 1995.

[Syn15] Synchrony. Synchrony company, 2015. [Accessed: 04-10-2015].

[WFDR+] FN Werfel, U FLOEGEL-DELOR, R ROTHFELD, T RIEDEL, D WIPPICH, and B GOEBEL. Flywheel energy storage system (fess) with hts magnetic bearings. *Energy [kWh]*, 2:5–7.

[ZNTZ10] Chi Zhang, TD Nguyen, KJ Tseng, and S Zhang. Stiffness analysis and levitation force control of the active magnetic bearing for a partially-self-bearing flywheel system. In *Sustainable Energy Technologies (ICSET), 2010 IEEE International Conference on*, pages 1–6. IEEE, 2010.